2-3 Trenching

2-3-1 Results of Trenching

Since the Area a-1 was considered to be promising, judging from the results of geological and geochemical (soil panning) surveys, trenching was carried out at 13 sites in the Area a-1, to clarify the extension of quartz veins and the relationship between the gold in soil and the geology.

Findings in the respective trenches were as follows:

Trench No. 1 (10 m long)

This trench was dug to confirm the 30 m south extension of quartz veins which are exposed along the riverbed. At a depth of about 2 m from the ground surface, bedrock of phyllite was encountered. The Au grades of six quartz veins (15 to 40 cm wide) in parallel to the schistosity of phyllite were 0.003 to 0.007 ppm.

As a result of panning, maximum 5 grains of gold (corresponding to 23.262 ppm Au in heavy mineral concentrate and 0.070 ppm Au in soil sample) were observed. The Au contents in the soil samples taken at 5 sites are 0.005 to 0.008 ppm.

Trench No. 2 (10 m long)

Trenching was carried out at the top of small hill to confirm the extension of quartz veins on 50 m south of the trench No. 1. Digging 2 m from the ground surface could not reach the bedrock, and by augering, it was found that the bedrock lay 3.0 to 3.5 m further below the trench bottom. Therefore, the trenching was given up. The highest Au grade on the side wall was only 0.014 ppm in heavy mineral concentrate and 0.004 ppm in soil.

Trench No. 3 (10 m long)

This trench was carried out at further 40 m south of trench No. 2. Thirty (30) m south from this trenching, there is a small valley, and several quartz veins are exposed on the riverbed.

At about 4 m below the ground surface, bedrock of phyllite and sandstone were encounted, and several narrow quartz veins (2 to 5 cm wide) were confirmed. On the bedrock, a gravelly portion contains pebbles of quartz (20 to 50 cm in size) and limonite (layer C), indicating that the soil has a little moved.

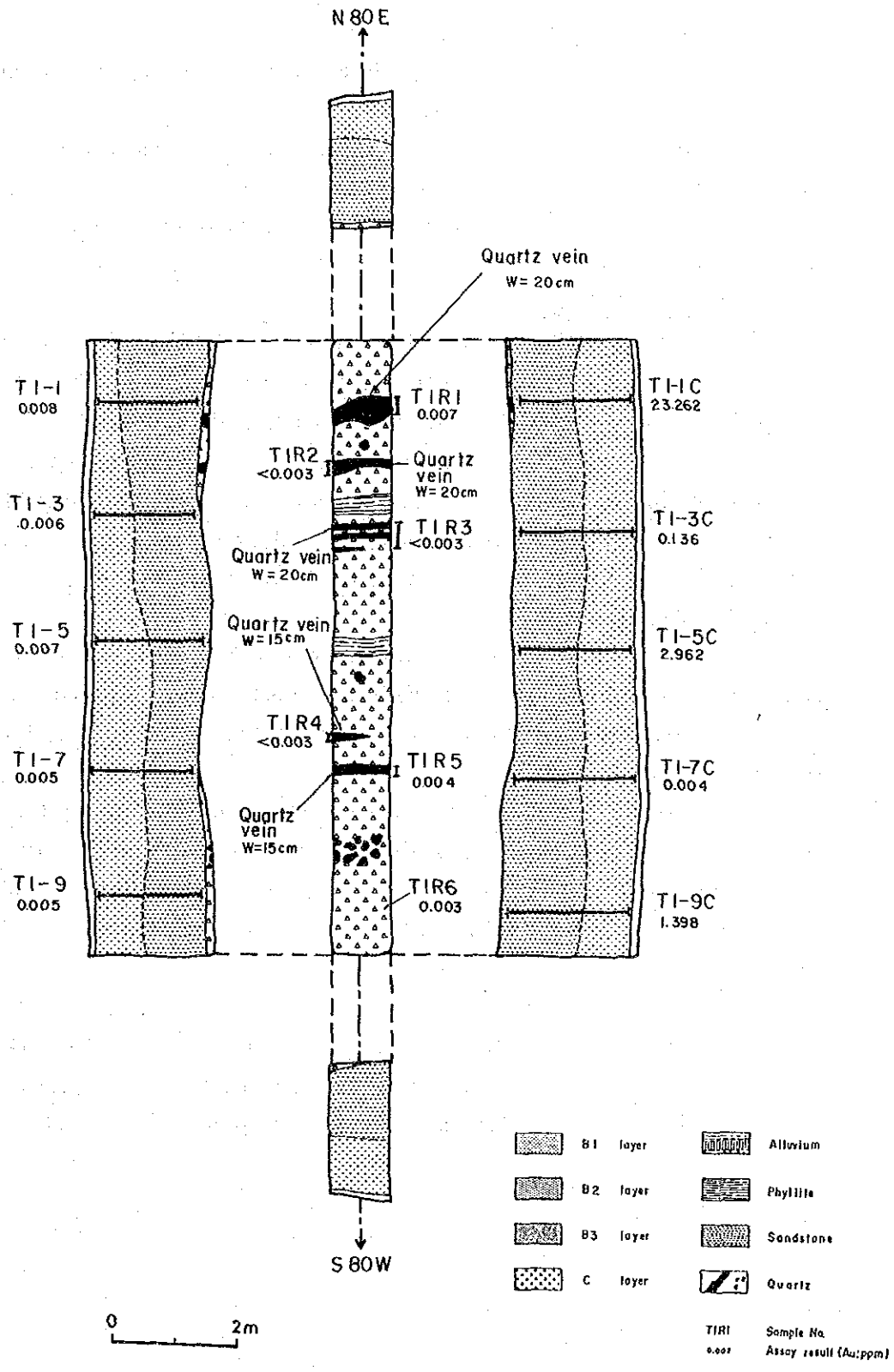

Trench 1

Fig. II - 2 - 7 Sketch map of trench 1 in the Area a-1

Trench No. 4 (10 m long)

This trench was carried out to confirm the extension of 30 m north of the quartz veins exposed on the riverbed.

This trench is located on the opposite slope of trench No. 1.

The phyllite bed was reached at a depth of about 2.5 m, and two quartz veins (5 cm wide each) were confirmed. Analytical values are low for both the quartz veins and soil.

Trench No. 5 (10 m long)

This trench is located at 50 m south of trench NO. 3. It was dug to confirm the extension of 5 m wide quartz vein exposed on the river bank to the south. The quartz is crystalline and contains no sulfide minerals.

At a depth of 2 m, bedrock of phyllite was reached, and a 2.5 m wide quartz vein was confirmed. The quartz vein itself contains few gold (0.004 ppm), but in the heavy mineral concentrate, the values are exceeded 1 ppm. The gold contents in soil are 0.003 to 0.004 ppm close to the detection limit.

Trench No. 6 (13 m long)

In the middle reaches of S. Jong, gold grains were confirmed by panning in strongly kaolinized and pyritized phyllite. To confirm the extension of the altered zone, trenching was carried out at two sites, north side (trench No. 6) and south side (trench No. 7) of S. Jong.

In trench No. 6, phyllite bedrock was reached at a depth of about 1.5 m from the ground surface. The phyllite has a schistosity of N50W and 65N, and contains lenticular quartz veins of 1 to 3 cm. It is remarkably kaolinized. The Au grades of outcrop and altered phyllite containing the quartz veins in the trench are as follows:

Sample No.	Width	Au	Remarks
Y-60	50 cm	2.00 ppm	Outcrop
TR6-1	150 cm	3.25 ppm	Trench No. 6

Trench No. 7 (9 m long)

This is located about 40 m south of trench No. 6. At a depth of about 1 m, phyllite bedrock was found. The phyllite is strongly kaolinized, and weakly phyritized. Quartz veins of 1 to 3 cm wide were confirmed.

However, unlike trench No. 6 on the opposite bank, quartz veins and phyllite in the trench showed low values close to the detection limit.

Trench No. 8 (10 m long)

Trenches Nos. 8 and 9 were dug to explore the Au geochemical anomalous zone found near the Main Range granite in the upper reaches of S. Jong. Due to poor exposures, trenching was considered to be an effective method for obtaining the geological information.

Trench No. 8 was dug on a road of a oil palm estate. When it was dug to a depth of 2.7 m from the ground surface, layer B appeared till the trench bottom. By augering, the bedrock was estimated to lie further 4 to 5 m below. The bedrock is heavily weathered and is a little difficult to identify. But it seems to be coarse grained quartz sandstone. The gold contents in heavy mineral concentrate are 6.91 to 14.19 ppm and those of soil were 1.61 to 3.57 ppm, comparatively high values.

Trench No. 9 (10 m long)

This trench is located at 50 m southeast of trench No. 8. Soil samples taken from this place contain gold grains.

At about 2 m from the ground surface, bedrocks of phyllite and sandstone were encountered. No quartz vein was observed. The schistosity of phyllite showed N50W and 35S. The sandstone is coarse grained and quartzose.

The Au contents in heavy mineral concentrate samples taken at 2 m intervals were 22.993 to 66.47 ppm and those of soil were 1.96 to 2.6 ppm, being the highest value compared with those in the other trenches.

Trench No. 10 (10 m long)

This trench was dug to confirm the Au geochemical anomaly found in the central south of the area. In valley, the south of the trench, kaolinized phyllite is exposed.

At about 2.5 m from the ground surface, phyllite was encountered. The phyllite showed a monoclinal structure of N50E and 50N, and bears several quartz veins (about 1 cm wide), being weakly kaolinized.

The Au contents in the quartz veins were less than 0.003 ppm, and that in the phyllite was 0.013 ppm. The maximum content of side wall soil was 0.182 ppm.

Trench No. 11 (3 m long)

This trench was dug using a backhoe at 50 m WSW Of trench No. 8. At this place, a large gold grain (23.4 mg) was confirmed in a soil sample obtained by augering, but since the weathered soil was too thick, trenching was given up.

Even 4.0 m digging from the ground surface could not reach the bedrock.

The soil gradually changed from yellowish brown to reddish brown according to the increase of depth. Rock fragments could not be found.

Analytical results were as listed below. It can be seen that the Au content increases towards depth.

Table II-2-2 Assay Results of Trench 11 Samples

Soil			Concentrate		
Sample No.	Depth	Au	Sample No.	Depth	Au
T111	0.20-3.20 m	0.661 ppm	T111c	0.20-1.20 m	0.312 ppm
			T112c	1.20-2.20	0.389
			T113c	2.20-3.20	4.542

Trench No. 12 (5 m long)

This trench was dug by a backhoe at 50 m ENE from trench No. 9.

In the trench, the soil was yellowish brown (layer B), from the ground surface to a depth of 2 m, and gradually increased the fragments of yellowish brown phyllite until yellowish brown bedrock of phyllite was reached at a 3 m depth.

Au content increases towards depth as in trench No. 11.

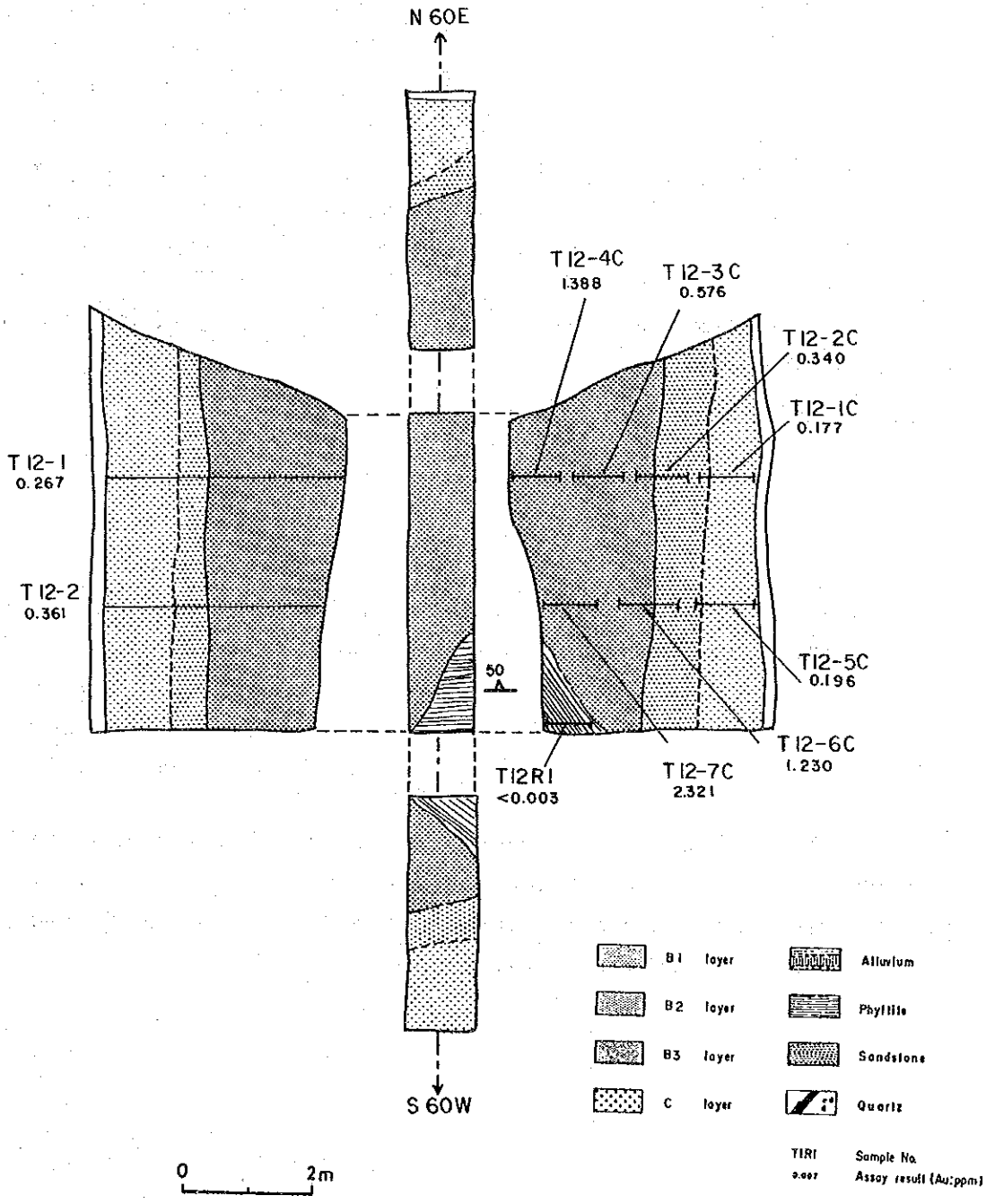

Trench 12

Fig. II - 2 - 8 Sketch map of trench 12 in the Area a-1

Table II-2-3 Assay Results of Trench 12 Samples

Soil			Concentrate		
Sample No.	Depth	Au	Sample No.	Depth	Au
T121	0.20-4.00 m	0.267 ppm	T121c	0.20-1.20 m	0.312 ppm
			T122c	1.20-2.20	0.340
			T123c	2.20-3.20	0.576
			T124c	3.20-4.20	1.388
T122	0.20-3.70	0.361	T125c	0.20-1.20	0.196
			T126c	1.20-2.20	1.230
			T127c	2.20-3.40	2.321

The bedrock of phyllite has a strike of N-S and a dip of 50E. No quartz vein could be confirmed.

Trench No. 13 (3 m long)

Table II-2-4 Assay Results of Trench 13 Samples

Soil			Concentrate		
Sample No.	Depth	Au	Sample No.	Depth	Au
T131	0.20-4.00 m	1.179 ppm	T131c	0.20-1.20 m	9.932 ppm
			T132c	1.20-2.20	4.432
			T133c	2.20-3.20	3.979
			T134c	3.20-4.20	4.089

The soil from the ground surface to a depth of 2.5 m is yellowish brown (layer B), and in the deeper section of soil, many pieces (max. 50 x 20 x 20 cm) of goethite were found. This trench was dug up to 4.2 m, the limit of the back hoe's capability, but the bedrock could not be reached.

2-3-2 Discussion

Trenching was carried out at 5 sites in the zone where quartz veins were densely observed in the center of this area, 2 sites in the mineralized zone in the middle reaches of S. Jong, and at 6 sites where gold grains were observed by geochemical soil survey (total trench length 113 m).

All trenches are in a rubber estate or oil palm estate, and are located on a gentle hilly area with 40 to 70 m above the sea level. For this reason, the thickness of weathered soil to the bedrock ranged from 2 to 5 m. Out of 13 trenches, 4 trenches could not reach the bedrock.

In the trenches of the quartz vein rich zone in the center, gold grains were observed only at one place on the trench side wall, and the quartz veins in the bedrock contained few gold.

In the trenches of mineralized zone, quartz veins in parallel to the schistosity of phyllite of the bedrock could be confirmed. The phyllite is strongly kaolinized and pyritized, and the Au content of the phyllite was 3.247 ppm in a sampling width of 1.5 m (trench No. 6). Henceforth, it is necessary to confirm to the extension of this altered zone.

In the 5 trenches dug near the boundary of Main Range granite in the east, Au contents were high, being 0.3 to 3.6 ppm in the soil samples taken in widths of 2 to 4 m, and 0.6 to 66.5 ppm in the heavy mineral concentrate samples taken in widths of 2 to 4 m. The anomalous zone shows a certain extent with good Au content which tends to increase towards depth from the ground surface. Therefore, this zone is considered high potential for Au deposit.

2-4 General Discussion on the Survey Results

The geochemical survey for soil has disclosed a distinct Au-As anomalous zone in the northeastern part of the area. This zone is in phyllite and located near the boundary of the Main Range granite. This anomalous zone covers an area of 0.6 km x 1.4 km = 0.8 km^2 with mean and maximum values of Au: 0.410 ppm and 2.708 ppm, respectively. The Au values at 5 trenching sites vary from 0.267 to 3.572, increasing towards depth.

As anomalies of Au, Zn, Sn and W overlap each other, mineralization of a high temperature type can be expected in this area.

Although the relation between mineralization and geology is not clear due to poor outcrops, it can be imagined from a linear extension of Au anomalies that in parallel to the granite boundary there is a structural line along which the Au mineralization has mainly taken place.

Another Au anomalous zone (area: 0.6km x 0.9km = 0.54km^2, mean value = 0.139 ppm, maximum value = 0.902 ppm) is also distributed in the phyllite zone in the southern central part of the area. Field evidences indicating existence of igneous rocks, such as hornfels, could not be found in the area. However, geological setting of the surrounding area suggests a possible stock of underground granite.

The mean and maximum values of Au anomalies are about 1/3 of those of the northeastern anomalies. The potential for Au deposit is, therefore, considered small.

In order to discover the source of gold flakes in the northern branch of the S. Jong in the central part, which was found by Phase I survey, detailed geological and geochemical surveys were carried out over its whole basin (0.5 km x 0.6 km = 0.30 km^2). The gold flakes could be traced up to the headstream for about 1 km, though they suddenly decreased in number towards upstream. However, few gold was contained in quartz vein outcrops, augered soil and trench's soil, due probably to the following reasons.

1 The Phase I samples happened to be collected at the gold accumulated sites.

2 Nuggets effect (unequal distribution) of gold
The whole sample (96 pcs of soil samples from a 100 m x 50 m grid pattern and many quartz veins) show very low Au grade, indicating low potential for Au deposit in the branch stream basin.

Chapter 3 Area a-2

3-1 Geological Survey

3-1-1 Geology

The Area a-2 is composed of Paleozoic Terolak Formation, the Main Range granite (which has intruded in the Terolak Formation), and the Quaternary Formation.

The Terolak Formation which occupies the eastern hill of the survey area, consists of black phyllite with clear schistosity, striking N30W and dipping 60W same as in the Area a-1.

The Quaternary formation is alluvium sediment distributed near the trunk road in the south. It is composed of fine-grained sand.

The granite, which is fine-grained and porphyrytic, is found on the northwestern hill. Judging from the distribution of its floats, it possibly occurs as a stock.

No large structural lines seem to be present.

3-1-2 Mineralization and Alteration

Neither mineralization nor alteration could be found in the area due to poor exposures. From the geology, gold bearing quartz veins are expected in the phyllite as same as in the Area a-1. The stream sediments in the small creek running on the north of the trunk road, contain a few gold flakes. On the east, placer tin was once mined, leaving a mine pond.

3-2 Geochemical Survey

3-2-1 Interpretation Results

The mean, minimum and maximum values of each element, correlation matrix among elements and EDA statistical values are given in Table II-3-1.

(1) Mean, Minimum and Maximum Values and Correlation Ratios

Comparing the mean value of each element of the whole sample population with that of alluvium - excluded sample population, Sn value of the former population is a little higher than that of the latter population. On the contrary, Zn and Au values of the panned sample of the former population are a little lower. The rest of the elements show almost same values.

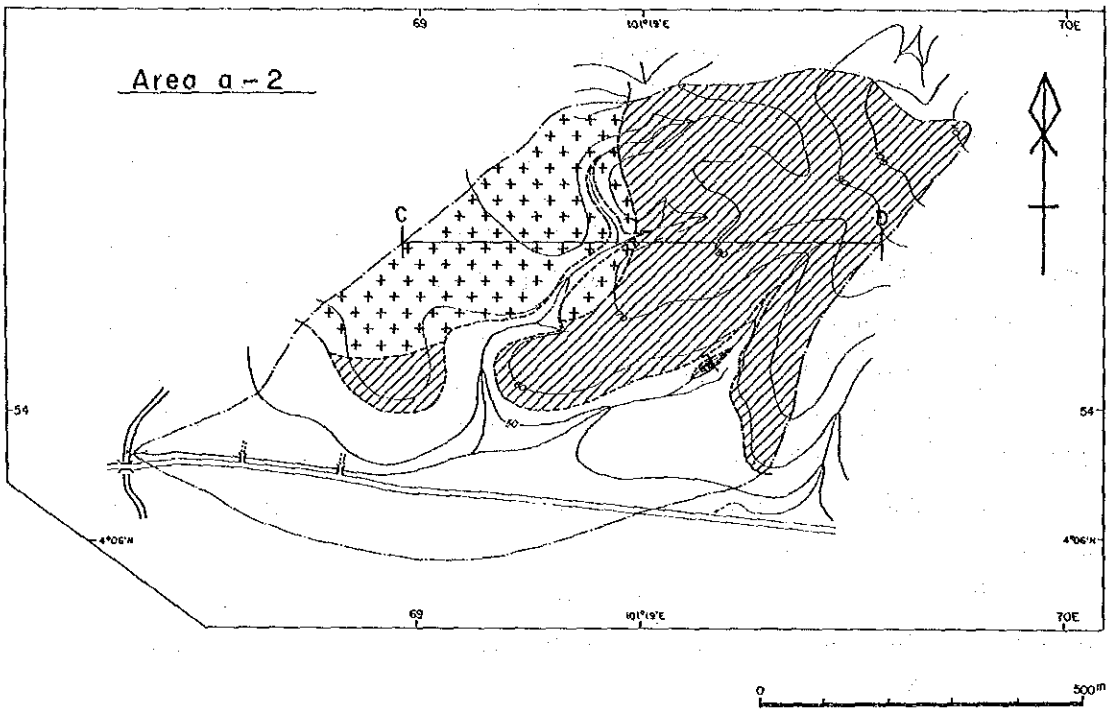

LEGEND

Quaternary Formation — Clay, sand, gravel

Teroiak Formation — Phyllite

(Intrusive Rocks)

Main Range Granite — Porphyritic granite

40 — Dip and strike of schistosity

Geological boundary

80 — Topographic contour (height in meter)

Survey area

A B — Section A-B

C D — Section C-D

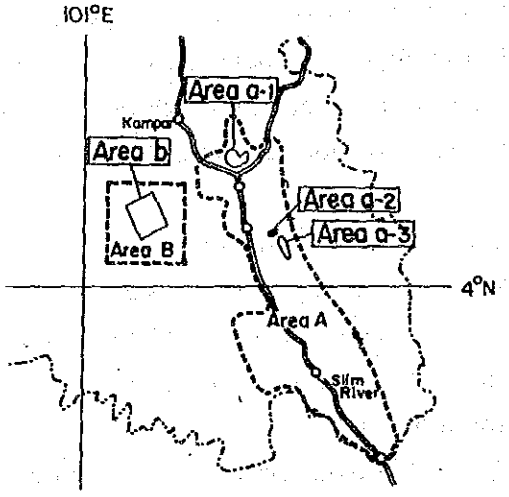

Fig. II - 3 - 1 . Geological map of the Area a-2

(1) Maximum, minimum and mean values (ppm)

	All Samples (34)				Pgt, Egt (17)			
element	Maximum	Minimum	Mean	S.D.	Maximum	Minimum	Mean	S.D.
Au	0.068	<0.003	0.005	0.582	0.068	<0.003	0.005	0.557
Ag	0.10	0.05	0.052	0.072	0.05	0.05	0.050	0.000
Pb	49	7	19.2	0.221	49	8	18.9	0.220
Zn	163	25	58.0	0.206	163	25	62.6	0.213
Cu	21	2	7.7	0.255	19	2	6.4	0.238
As	200	5	20.7	0.407	200	5	19.2	0.347
W	20	4	10.3	0.142	20	4	10.4	0.164
Sn	180	5	15.4	0.495	40	5	9.4	0.325
conc-Au	0.415	<0.003	0.007	0.861	0.415	<0.003	0.013	0.964

Pgt; Porphyritic granite Egt; Equigranular granite

(2) Correlation matrix

Soil samples except for alluvium samples

	Au	Ag	Pb	Zn	Cu	As	W	Sn	conc-Au
Au	1.000								
Ag	.001	1.000							
Pb	.250	-.002	1.000						
Zn	.071	-.002	.142	1.000					
Cu	.056	-.003	.240	.267	1.000				
As	.666	-.001	.432	.344	.175	1.000			
W	.176	-.001	.588	.431	.286	.343	1.000		
Sn	-.007	-.001	-.097	.308	-.078	.018	.595	1.000	
conc-Au	.255	.002	.175	-.158	.361	-.076	.202	.327	1.000

All soil samples

	Au	Ag	Pb	Zn	Cu	As	W	Sn	conc-Au
Au	1.000								
Ag	-.077	1.000							
Pb	.072	.220	1.000						
Zn	-.008	.150	.392	1.000					
Cu	.336	.124	.044	-.081	1.000				
As	.495	.209	.167	-.003	.560	1.000			
W	.184	.074	.366	.267	.212	.307	1.000		
Sn	.205	.238	-.111	-.203	.544	.538	.289	1.000	
conc-Au	.061	-.181	.035	-.066	.052	-.163	.158	-.086	1.000

(3) Result of EDA

Soil samples except for alluvium samples (ppm)

	Au	Ag	Pb	Zn	Cu	As	W	Sn	conc-Au
MAXIMUM	0.068	0.05	49	163	19	200	20	40	0.415
U.FENCE	0.013		33	140	12.5	47.5	18	17.5	0.086
U.WHISKER	0.006		21	79	8	25	12	10	0.035
U.HINGE	0.006		21	79	8	25	12	10	0.035
MEDIAN	0.004		18	67	5	20	12	10	0.005
L.HINGE	0.001		13	38	5	10	8	5	0.001
L.WHISKER									
L.FENCE	-0.006		1	-23.5	0.5	-12.5	2	-2.5	-0.050
MINIMUM	<0.003	0.05	8	25	2	5	4	5	<0.003

All soil samples (ppm)

	Au	As	conc-Au
MAXIMUM	0.068	200	0.415
U.FENCE	0.019	60	0.041
U.WHISKER	0.009	30	0.035
U.HINGE	0.008	30	0.017
MEDIAN	0.004	15	0.004
L.HINGE	0.001	10	0.001
L.WHISKER	0.001	10	0.001
L.FENCE	-0.01	-20	-0.023
MINIMUM	<0.003	5	<0.003

(4) Result of factor analysis

Factor loading and communality

	Factor 1	Factor 2	Factor 3	Communality
Au	-0.823	-0.017	-0.040	0.6795
Pb	-0.270	-0.061	-0.713	0.5849
Zn	-0.134	-0.481	-0.273	0.3234
Cu	-0.031	-0.063	-0.461	0.2178
As	-0.764	-0.141	-0.311	0.6998
W	-0.155	-0.668	-0.506	0.7263
Sn	0.038	-0.806	0.134	0.6689

Factor contribution (%)

Factor 1	Factor 2	Factor 3
57.655	28.575	15.692

Table II - 3 - 1 Statistical values of each element in the Area a-2

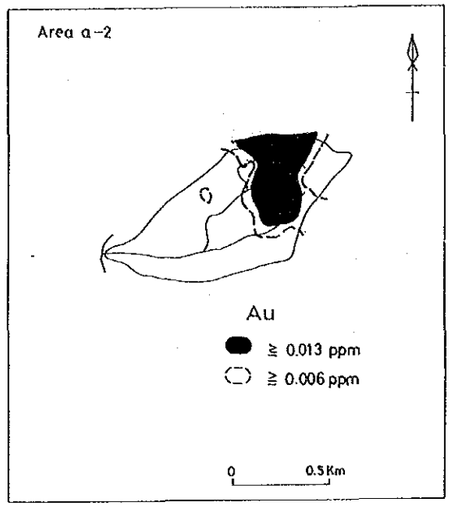

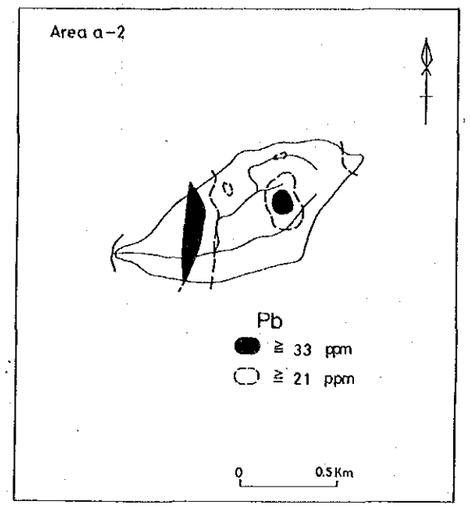

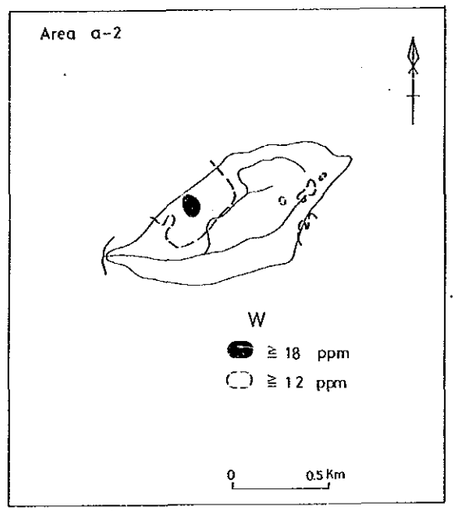

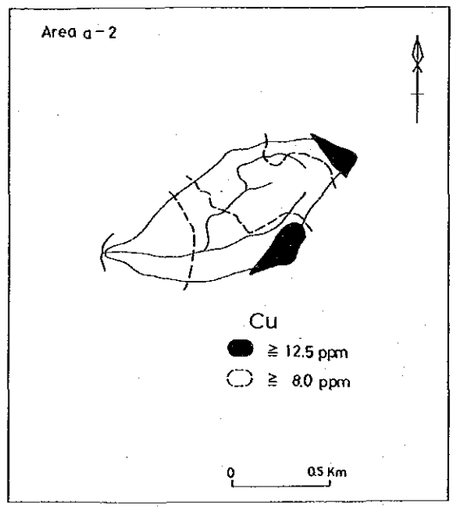

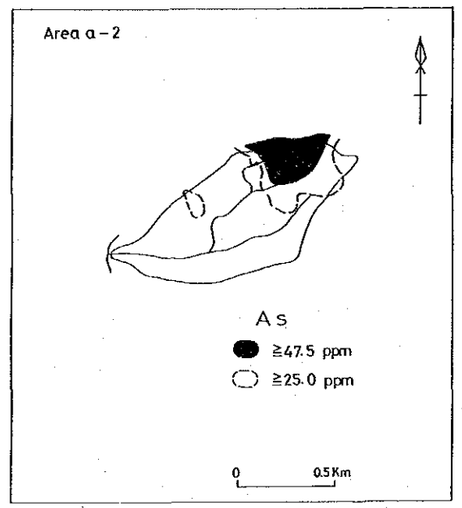

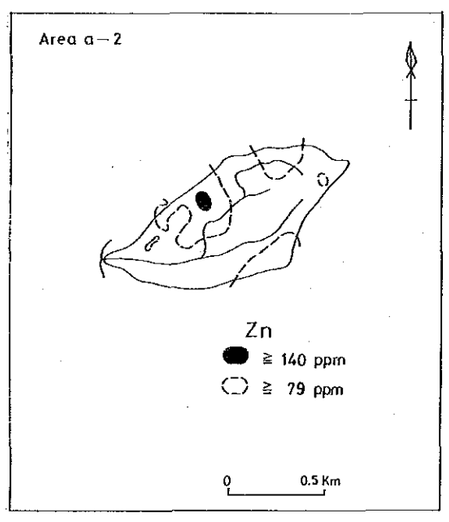

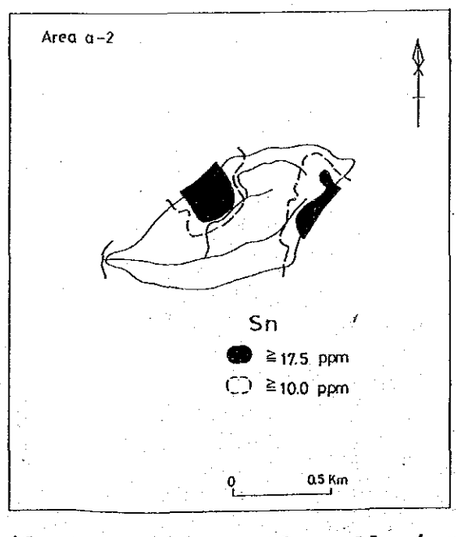

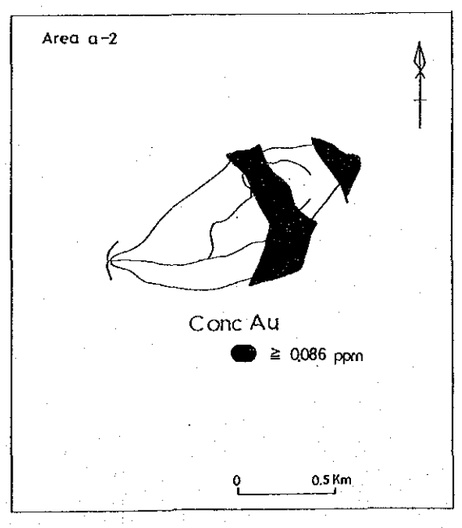

(Soil samples except for alluvium samples)

Fig. II - 3 - 2 Distribution map of elements in soil samples (Area a-2) (1)

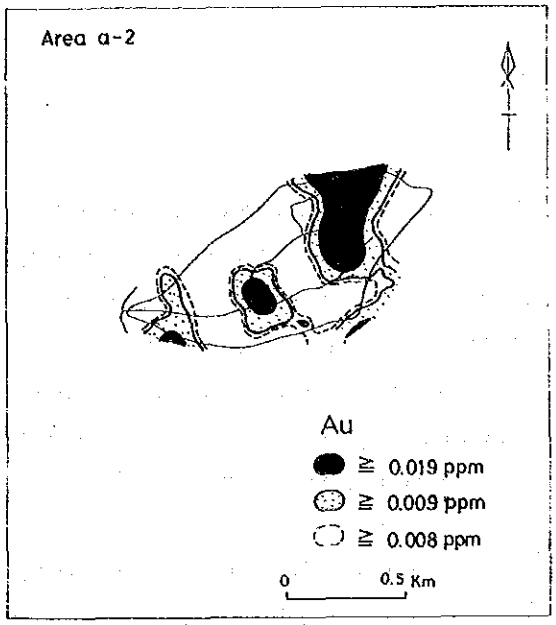

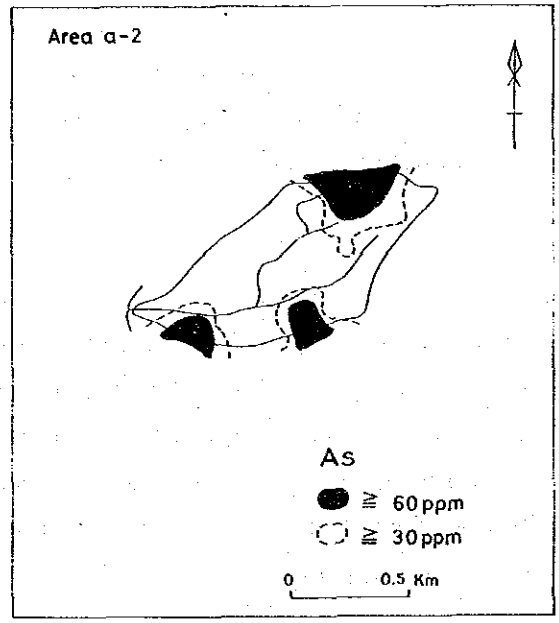

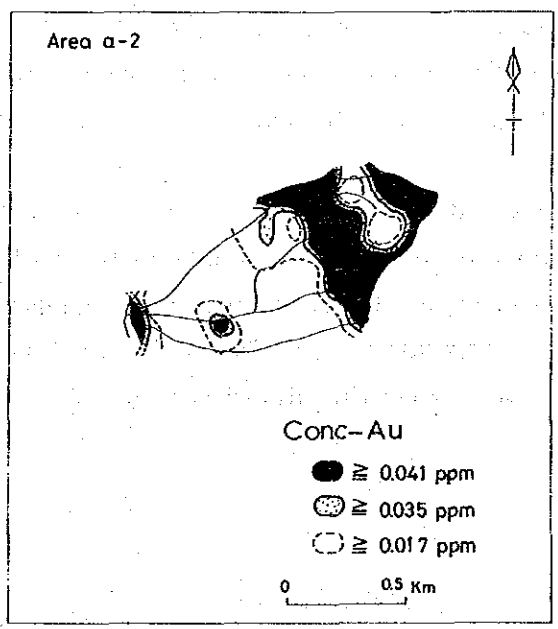

(All samples)

Fig. II–3–2 Distribution map of elements in soil samples (Area a-2) (2)

The correlation ratios of As-Cu (0.560), Sn-Cu (0.544), Sn-As (0.538) and As-Au (0.495) are relatively high in the whole sample population, while Au-As (0.666), Sn-W (0.595), W-Pb (0.588) and W-Zn (0.431) are higher in the alluvium - excluded samples population. Few high correlation ratios found among same elements in the two populations may be caused by mixing up of samples belonging to different categories, such as soil and alluvium.

(2) EDA Interpretation results

A distribution map for each element was constructed. However, Ag map was not made because all the statistical values are same as 0.050 ppm.

Elements of Au (in soil), As and Au in concentrate were processed separately for the whole sample population and for alluvium-excluded sample population.

Au

[1] Soil Samples

The anomalous values over the upper fence (Au=0.013 ppm) in the alluvium - excluded sample population are widely distributed in the central part of the area, locating near the boundary between granite and phyllite. Anomalous values in the whole sample population are found in the same above-mentioned place and also in the southeastern and southwestern areas. The anomalies in the latter two areas indicate gold concentration in the alluvial deposits.

[2] Concentrate Samples

Anomalous values over upper fence in the alluvium-excluded sample population are distributed in the central part as same as in another population. They tend to extend along a NW-SE direction.

As

The anomalous values over the upper fence in the alluvium - excluded sample population are widely distributed in the central part, partly overlapping the Au anomalies. Anomalous values in the whole sample population are found in the southeastern and southwestern parts, occupying almost the same Au area.

Other Elements

The following features can be noticed in the anomaly distribution of each element.

The wide anomalous zone of Au-As in the central part of the Area a-2 contains a part of Pb anomalous zone. The Zn anomalies are located on the southeastern and southwestern parts of the Au-As anomalous zone and the Cu anomalies, on the northeastern and southern parts of the anomalous zone, as if they surrounded the Au-As zone. The Sn anomalous zone in the southwestern part includes a part of Zn and W anomalous zones.

(3) Multivariate Analysis

Through factor analysis for the alluvium-extracted sample population (N=17pcs), the following 3 factors were extracted as shown in Table II-3-1. The contribution of Factor 1 and Factor 2 are 57.7% and 28.6%, respectively.

As the sum of two figures amounts to 86%, Factor 1 and Factor 2 will be discussed.

Factor 1 (Au-As)

All the Factor 1 loading values are negative except for Sn. Elements of Au and As have large negative values, indicating an effect of Au mineralization. Factor scores negatively higher than -1.0 are found in the northeastern part of the area. They are detected in the phyllite zone on the east of granite stock, extending in the N-S direction.

Factor 2 (W-Sn-Zn)

All the Factor 2 loading values are negative. Among them, W, Sn, (Zn) values are negatively large, which indicate an effect of Sn, W mineralization. As shown in factor score map, high scores are both distributed in the eastern phyllite zone and in the eastwestern granite zone, occupying the same area of Sn anomalies in the EDA interpretation.

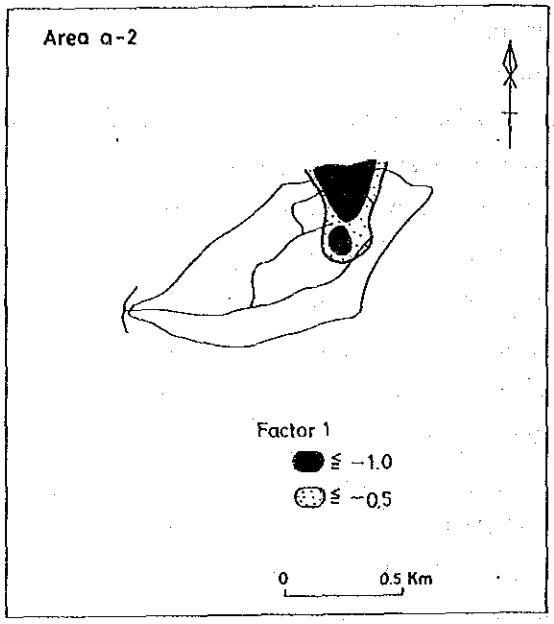

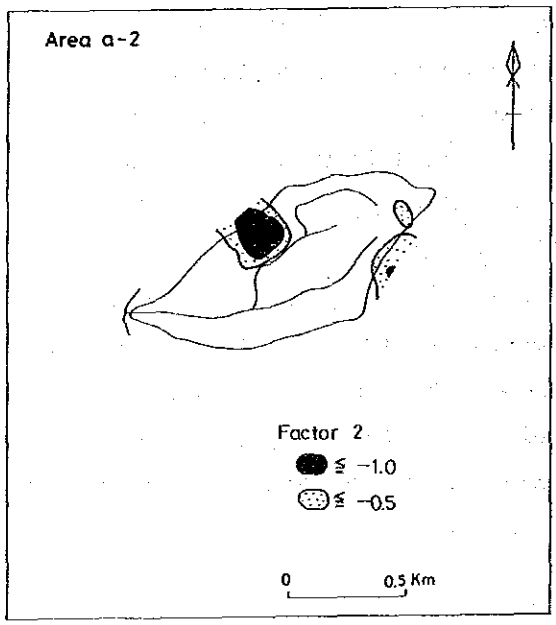

Fig. II - 3 - 3 Factor analysis map in the Area a-2

3-2-2 Discussion

As the soil samples are only 17 pieces, it is a little qustionable to process statistically their geochemical data. However, it can be said as a general trend that geochemical anomalies of Au and As are distributed in the phyllite zone on the east of granite stock as if they surrounded the stock, while anomalies of Cu, Zn, Sn and W are located around the Au-As anomalies. The granite stock is distant 2km from the Main Range granite. Between these two granites, 4 operating tin mines and some placer tim mines are known. Therefore, the geochemical anomalies obtained in this phase is possibly closely related to the tin mineralization.

3-3 Overall Discussion on the Survey Results

Geological and Geochemical surveys disclosed granite intrusion and geochemical Au-As anomaly in the phyllite on the east of the granite.

The Au anomalies cover an area of 0.3km x 0.5km = 0.15km^2 with mean value of 0.039ppm and maximum value of 0.086ppm, which correspond respectively to 1/4 and 1/13 those of the Area a-1 anomalies.

Relationship between geochemical anomalies and geology were not well clarified due to poor exposures.

In order to seek for the source of gold nuggets (about 100mg) found in the creek in the southwestern area, soil samples were systematically collected and analyzed, resulting no high geochemical anomalies of Au. Some favorable conditions for mineral exploration, such as granite intrusion and geochemical anomalies are present. However, from the values of the anomalies the mineralization seems to be weak, therefore, the follow up survey is not necessary.

Chapter 4 Area a-3

4-1 Geological Survey

4-1-1 Geology

Almost whole area is occupied by the Terolak Formation of Poleozoic, which consists of black phyllite and silty phyllite, striking N20W and dipping 50 - 80W.

Quaternary sediment is mainly composed of mine dump, which is distributed narrowly from the middle reaches to the lower reaches of S. Chebor.

The Main Range granite boundary lies about 1km east away from the area, where no granite intrusion were recognized.

Judging from its straight extension and topographical contrast, S. Chebor is considered to be a tectonic valley.

4-1-2 Mineralization and Alteration

An abandoned mine probably for primary tin was found at the middle course of S. Chebor. A trough with 50 - 150m width, 400^{m} length and 20m height is the remains of ex-mine workings, that were reportedly operated for Sn and Au (by-product). A small sericite zone and a few quartz veins (vein width 3 - 10cm) can be observed at the workings.

The Au grade of quartz vein is lower than 0.003ppm. Quartz veins from 1 to 10cm in width are commonly observed in the phyllite, however, they are almost barren.

4-2 Geochemical Survey

4-2-1 Interpretation Results

Mean, minimum and maximum values for each element, correlation matrix among elements and EDA statistical values are given in Table II-4-1.

(1) Mean, Minimum and Maximum Values and Correlation Ratios

Comparing the mean value for each element of the whole sample population with that of alluvium-excluded sample population, it is clear that these statistical values are almost same for each element. This is due to small number of samples (12%) of alluvium.

The relatively high correlation ratios are Au (soil) - Au (concentrate) (0.435), Sn-As (0.353), Cu-Pb (0.330) and Au-Pb (0.322) in the alluvium-

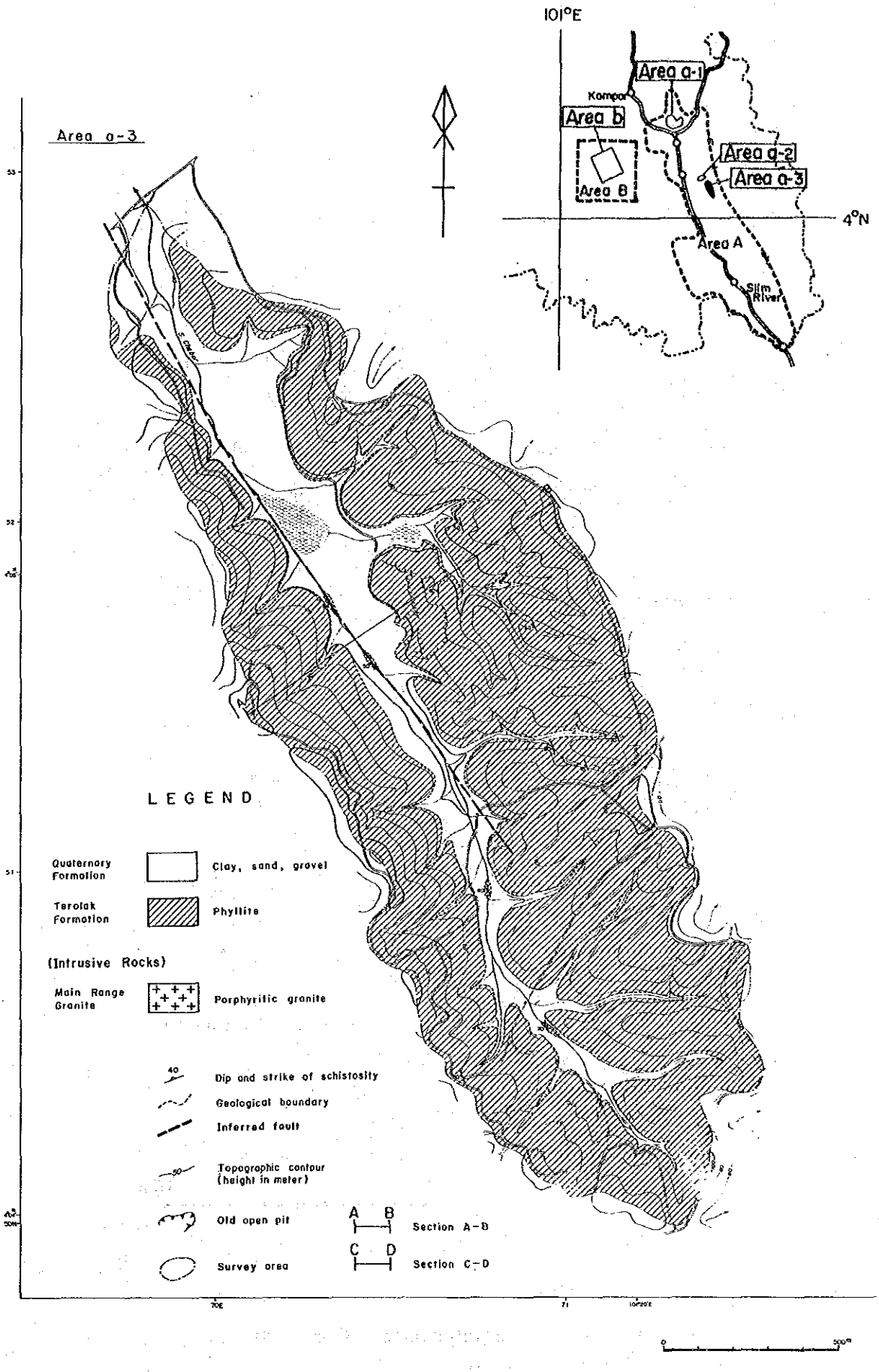

Fig. II - 4 - 1 Geological map of the Area a-3

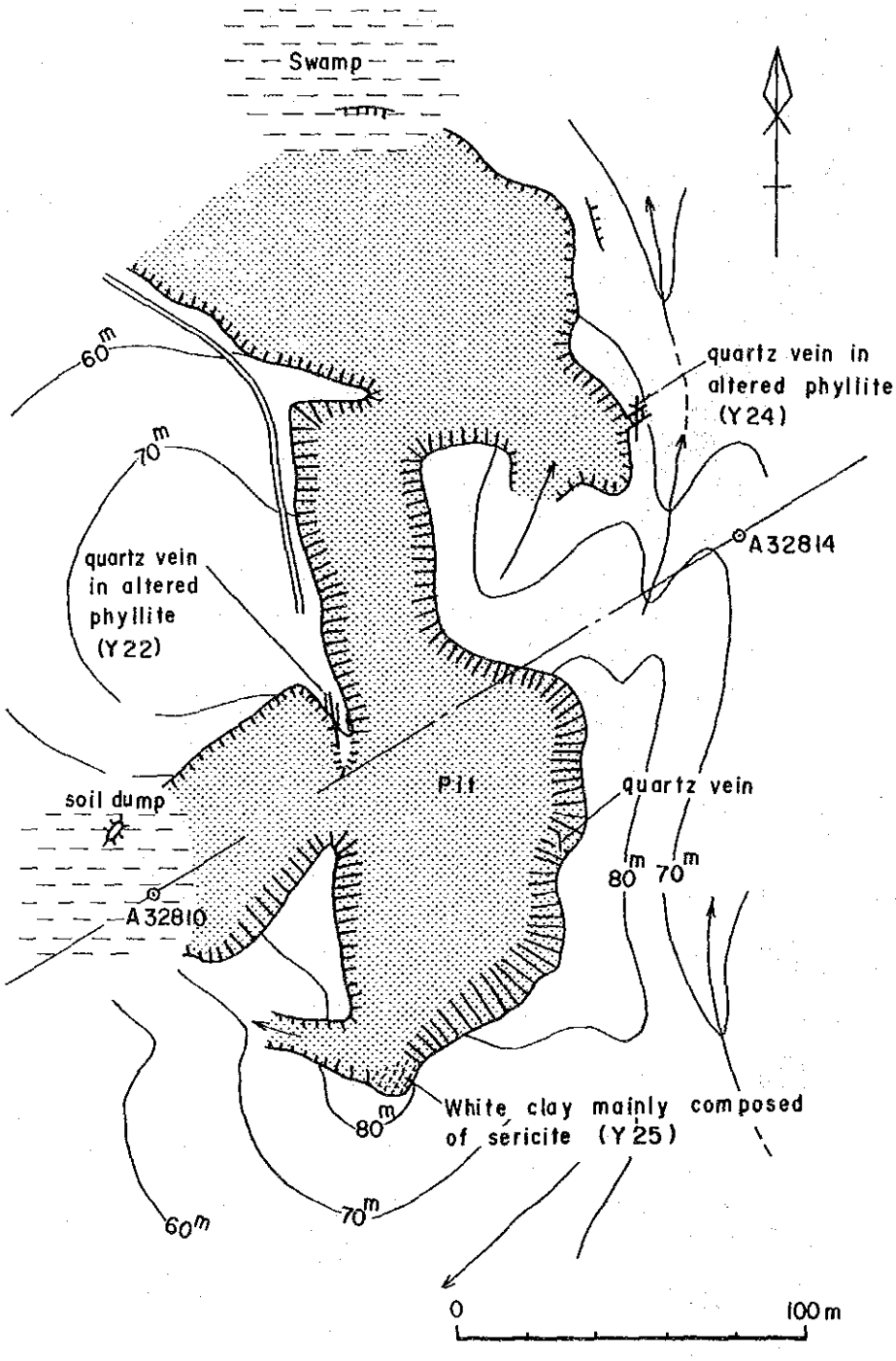

Fig. II - 4 - 2 Sketch map of old open-pit

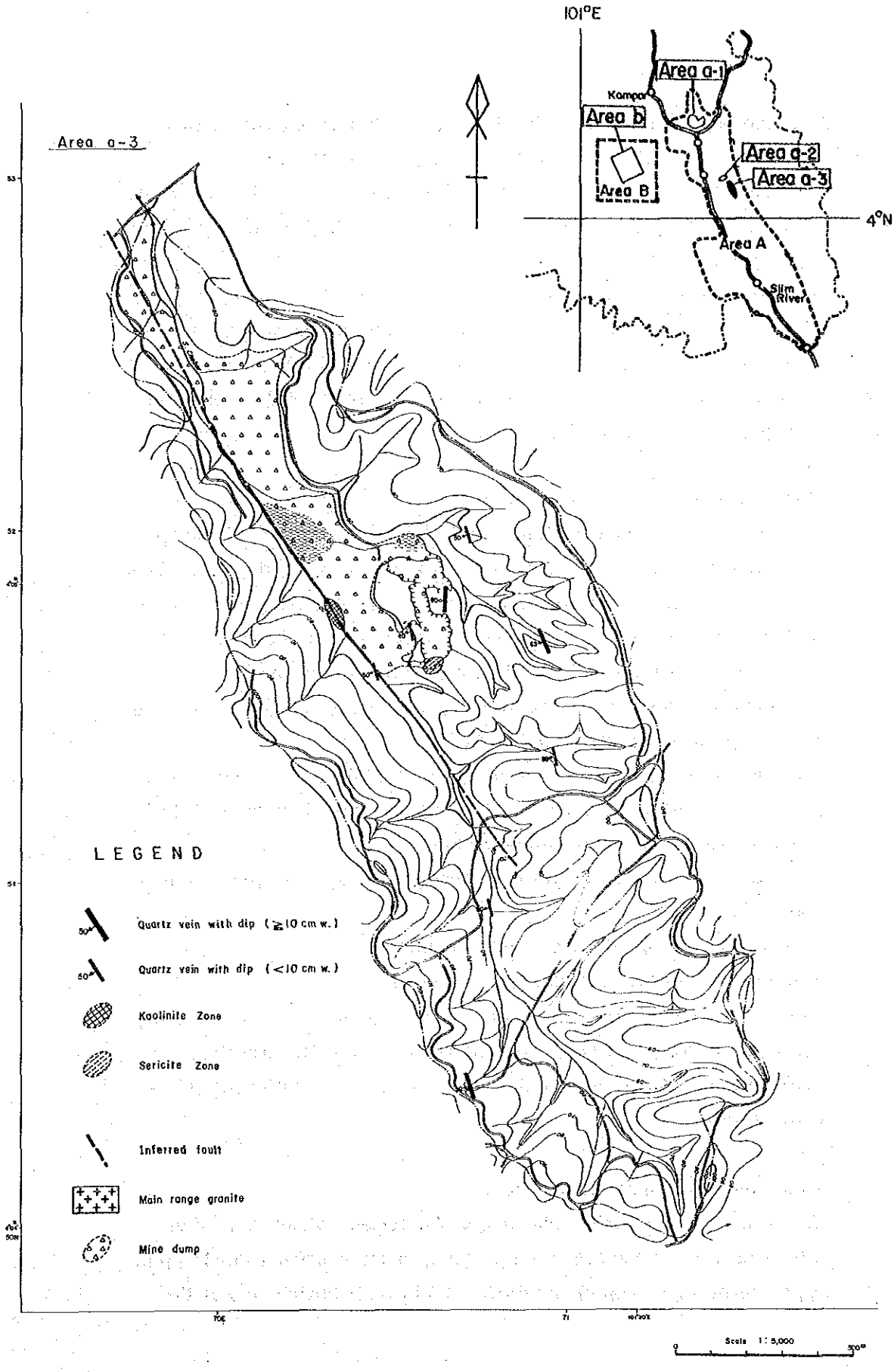

Fig. II - 4 - 3 Distribution map of the quartz veins and alteration zones in the Area a-3

excluded sample population and Cu-Pb (0.507), Au-Cu (0.498), Au-Pb (0.421), Pb-Zn (0.414) and Cu-As (0.391) in the whole sample population.

The correlation ratios of Au-As are high in the Area a-1 and a-2 but low in the Area a-3. On the contrary, Cu-Pb value is high in the Area a-3 unlike in the Area a-1 and a-2.

(2) EDA Interpretation Results

Elements of Au (in soil), Pb, As and Au (in concentrate) were processed separately for the whole sample population and alluvium-excluded sample population. Other elements were processed for only alluvium-excluded sample population.

Au

[1] Alluvium-excluded Polulation

Au values range from minimum =0.033ppm to maximum=0.339ppm. More than 80% of the samples are less than 0.024ppm in grade. The boxplot is truncated towards low grade. The maximum value of 0.339ppm is much lower than that (2.708ppm) in the Area a-1.

Analytical values were divided into 3 classes (upper fence= 0.036ppm, upper whisker=0.21ppm and upper hinge=0.015) and illustrated in Distribution Map of Au.

The anomalies over the upper fence are widely distributed on both sides of S. Chebor. The anomalous zones extend along a NW-SE direction, covering the old mine workings.

The same distribution pattern is recognizable in the whole sample population.

[2] Alluvium-excluded Concentrate Population

Minimum = 0.003ppm, maximum = 64.49ppm

The Au anomalies over upper fence (0.501ppm) are widely distributed along S. Chebor, extending in a NW-SE direction. The distribution pattern is similar to the above-mentioned [1] Au distribution.

Pb

Minimum=4ppm, maximum=43ppm

The boxplot has a little wide range. Analytical values were divided into 3 classes (upper fence = 19.5 ppm, upper whisker = 0.021 ppm, upper hinge = 0.015 ppm) and illustrated in Distribution Map of Pb.

(1) Maximum, minimum and mean values (ppm)

	All Samples (132)				Phy (116)			
element	Maximum	Minimum	Mean	S.D.	Maximum	Minimum	Mean	S.D.
Au	0.339	<0.003	0.007	0.663	0.339	<0.003	0.006	0.642
Ag	0.10	0.05	0.051	0.045	0.10	0.05	0.051	0.048
Pb	43	3	9.4	0.172	43	4	9.6	0.161
Zn	412	16	47.8	0.225	412	16	48.8	0.227
Cu	49	1	5.4	0.440	49	1	5.5	0.451
As	200	5	17.1	0.319	200	5	18.1	0.331
W	16	4	8.1	0.057	16	4	8.1	0.051
Sn	510	5	6.5	0.236	510	5	6.6	0.247
conc-Au	64.490	<0.003	0.036	1.389	64.490	<0.003	0.027	1.380

Phy; Phyllite

(2) Correlation matrix

Soil samples except for alluvium samples

	Au	Ag	Pb	Zn	Cu	As	W	Sn	conc-Au
Au	1.000								
Ag	-.122	1.000							
Pb	.322	-.084	1.000						
Zn	.037	.042	.069	1.000					
Cu	.061	.058	.330	.017	1.000				
As	-.022	.017	.190	-.321	-.109	1.000			
W	.115	.169	.266	-.043	.059	.134	1.000		
Sn	.134	-.078	.017	-.035	-.131	.353	.078	1.000	
conc-Au	.435	-.146	.221	-.116	.132	-.024	.068	.029	1.000

All soil samples

	Au	Ag	Pb	Zn	Cu	As	W	Sn	conc-Au
Au	1.000								
Ag	-.119	1.000							
Pb	.309	-.065	1.000						
Zn	.042	.046	.133	1.000					
Cu	.097	.060	.350	.012	1.000				
As	-.045	.028	.197	-.278	-.077	1.000			
W	.072	.146	.263	-.039	.032	.119	1.000		
Sn	.099	-.073	.042	-.042	-.115	.346	.074	1.000	
conc-Au	.451	-.150	.186	-.081	.114	-.074	.065	-.007	1.000

(3) Result of EDA

Soil samples except for alluvium samples (ppm)

	Au	Ag	Pb	Zn	Cu	As	W	Sn	conc-Au
MAXIMUM	0.339	0.10	43	412	49	200	16	510	64.490
U.FENCE	0.036		19.5	105.5	23	35	8	17.5	0.501
U.WHISKER	0.021		12	66	15	25	8	10	0.651
U.HINGE	0.015		12	62	11	20	8	10	0.201
MEDIAN	0.006		10	52.5	4	15	8	5	0.008
L.HINGE	0.001		7	33	3	10	8	5	0.001
L.WHISKER	0.001		7	27	2	10	8	5	0.001
L.FENCE	-0.020		-0.5	-10.5	-9	-5	8	-2.5	-0.299
MINIMUM	<0.001	0.005	4	16	1	5	4	5	<0.003

All soil samples (ppm)

	Au	As	As	conc-Au
MAXIMUM	0.339	43	200	64.490
U.FENCE	0.041	17	35	0.949
U.WHISKER	0.022	12	25	0.657
U.HINGE	0.017	11	20	0.380
MEDIAN	0.006	9	15	0.018
L.HINGE	0.001	7	10	0.001
L.WHISKER	0.001	7	10	0.001
L.FENCE	-0.023	1	-5	-0.568
MINIMUM	<0.003	3	5	<0.003

(4) Result of factor analysis

Factor loading and communality

	Factor 1	Factor 2	Factor 3	Factor 4	Communality
Au	0.485	-0.127	0.174	-0.174	0.3210
Ag	-0.092	-0.024	-0.078	0.433	0.2028
Pb	0.648	0.057	-0.016	0.061	0.4268
Zn	0.059	-0.568	-0.022	0.036	0.3280
Cu	0.401	0.029	-0.395	0.078	0.3236
As	0.115	0.506	0.382	0.112	0.4279
W	0.312	0.068	0.121	0.403	0.2793
Sn	0.096	0.135	0.569	-0.032	0.3522

Factor contribution (%)

Factor 1	Factor 2	Factor 3	Factor 4
41.658	34.907	18.940	13.031

Table II - 4 - 1 **Statistical values of each element in the Area a-3**

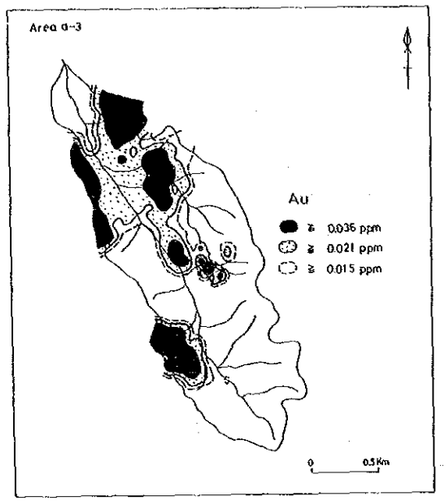

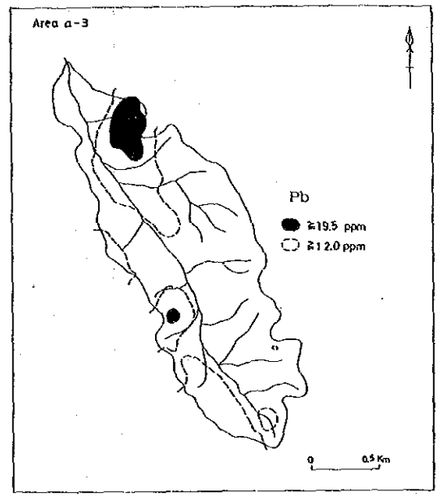

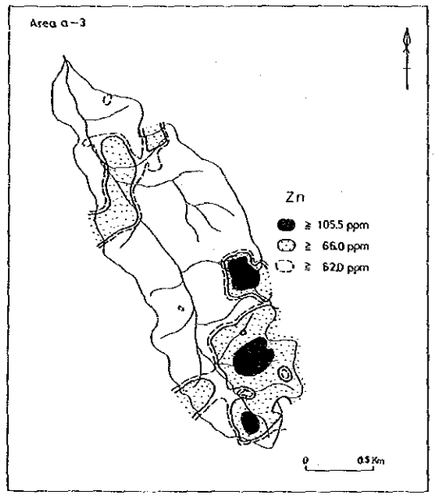

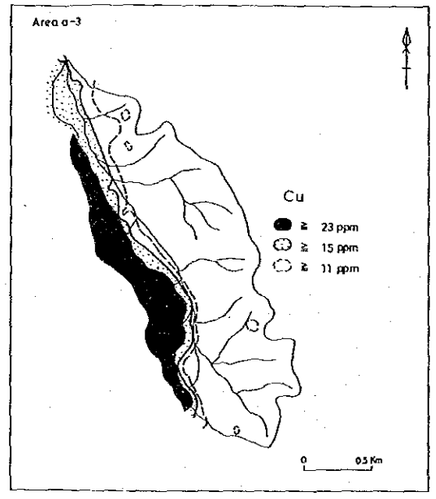

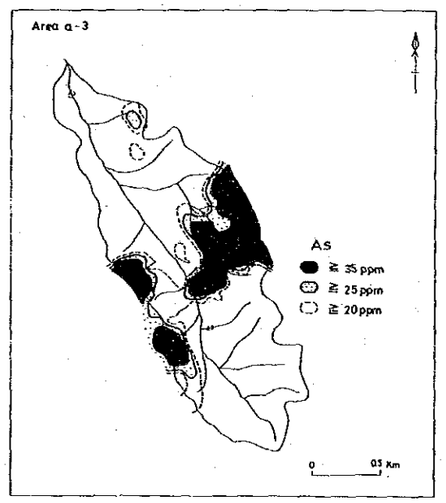

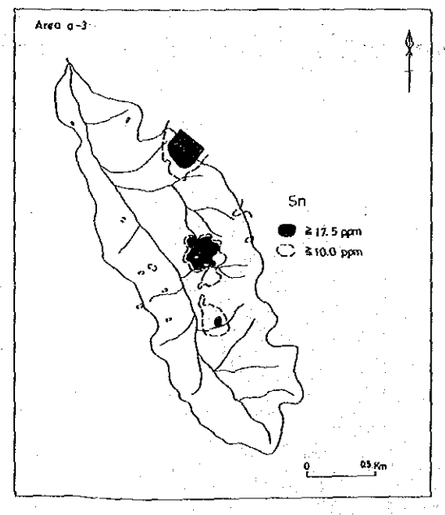

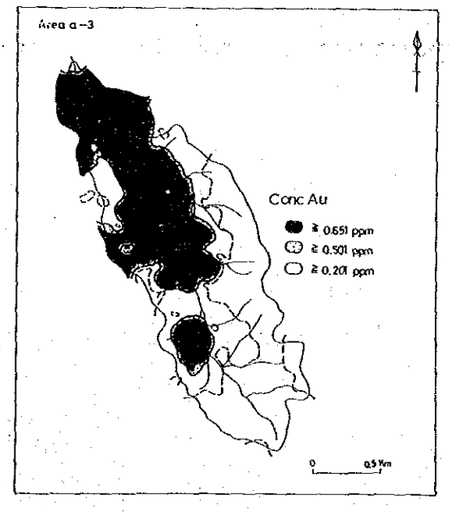

(Soil samples except for alluvium samples) (All samples)

Fig. II - 4 - 4 Distribution map of elements in soil samples (Area a-3) (1)

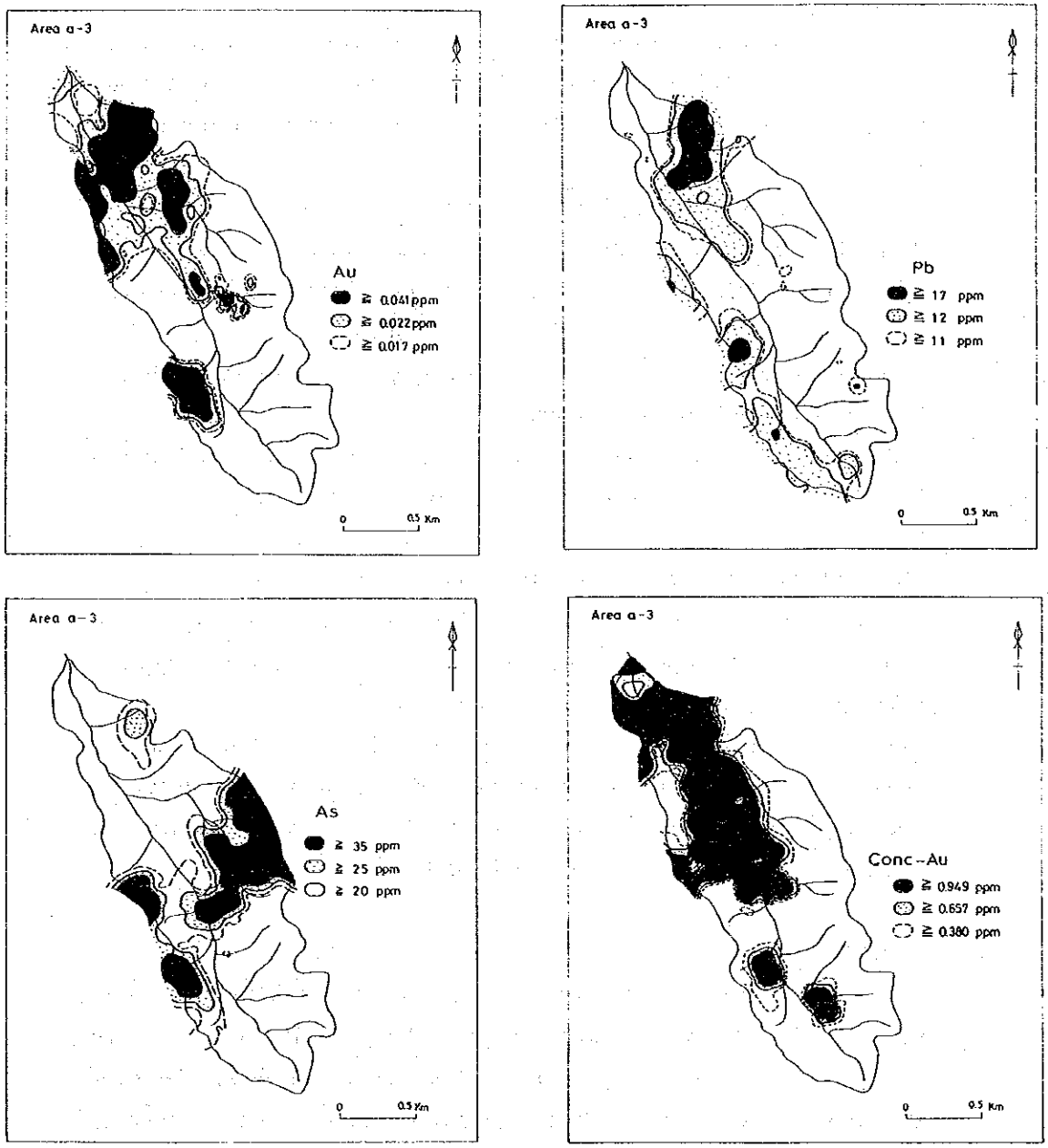

(All samples)

Fig. II–4–4 Distribution map of elements in soil samples (Area a-3) (2)

The anomalies over the upper fence are located in the middle to lower courses of S. Chebor.

The same pattern of Pb anomaly is obtained from the whole sample population being distributed along the lower course of S. Chebor and at 3 sites on the western mountain in the central part of the area.

Zn

Minimum value = 16 ppm, Maximum value = 412 ppm.

Analytical values were divided into 4 classes (upper fence = 105.5 ppm, upper whisker = 66 ppm, upper hinge = 62 ppm, lower hinge = 33 ppm and illustrated in Distribution Map of Zn.

The anomalies over the upper fence are sporadically scattered in the area from central to southern areas.

Unlike other elements, high Zn concentration tends to be distributed in a NE-SW direction rather than in a NW-SE direction.

Cu

Minimum value = 1 ppm, maximum value = 49 ppm.

Analytical values were divided into 4 classes (upper fence = 23 ppm, upper whisker = 15 ppm, upper hinge = 11 ppm and lower hinge = 3 ppm) and illustrated in Distribution Map of Cu.

The anomalies over the upper fence are distributed only on the western bank of S. Chebor, extending widely in a NW-SE direction. Judging from topography and geochemical anomaly pattern, S. Chebor is considered to be a tectonic valley.

As

Minimum value = 5 ppm, maximum value = 200 ppm.

Analytical values were divided into 4 classes (upper fence = 35 ppm, upper whisker = 25 ppm, upper hinge = 20 ppm, lower hinge = 10 ppm), and illustrated in Distribution Map of As. The anomalies over the upper fence are widely distributed in the central part, extending along a NE-SE direction.

Sn

Minimum value = 5 ppm, maximum value = 510 ppm.

More than 98% of analytical values are lower than 38.667 ppm. The boxplot is truncated to the lower values. Analytical values were divided into 3 classes (upper fence = 17.5 ppm, upper hinge = 10 ppm and lower hinge 5 ppm) and illustrated in Distribution Map of Sn.

One anomaly over the upper fence was found at one point on the soutern extension of old tin workings in the central part and anoter in the northeastern part. However, the relationship between anomalies and geology were not clear enough because of no exposures.

(3) Maltivariate Analysis

Through factor analysis for the alluvium-excluded sample population (N = 116 pcs), the following 4 factors were extracted as shown in Table II-4-1. The contributions of Factor 1, Factor 2 and Factor 3 are 41.6%, 34.9% and 18.9% respectively. As the total contribution of these three factors reaches 95%, Factor 1, 2 and 3 are discussed in this section.

Factor 1 (Pb - Au - (Cu))

The elements with large loading values of Factor 1 are Pb, Au and Cu, which suggests an effect of mineralization of these elements.

Factor 1 score map is shown as Fig. II-4-5.

High score zones are distributed in phyllite in the western side of the Area a-3.

Comparing this map with EDA interpretation map for Au and Cu, the Factor 1 score map looks like a composed map of the anomalies of two elements. The high score zone extends parallel to S. Chebor (in NNW - SSE direction).

Factor 2 (Zn, As)

Among the Factor 2 values obtained for the elements, As has a large positive value but Zn has large negative value. The factor score map shows large negative scores. The Zn anomaly map made by EDA interpretation is quite similar to the Factor 2 map.

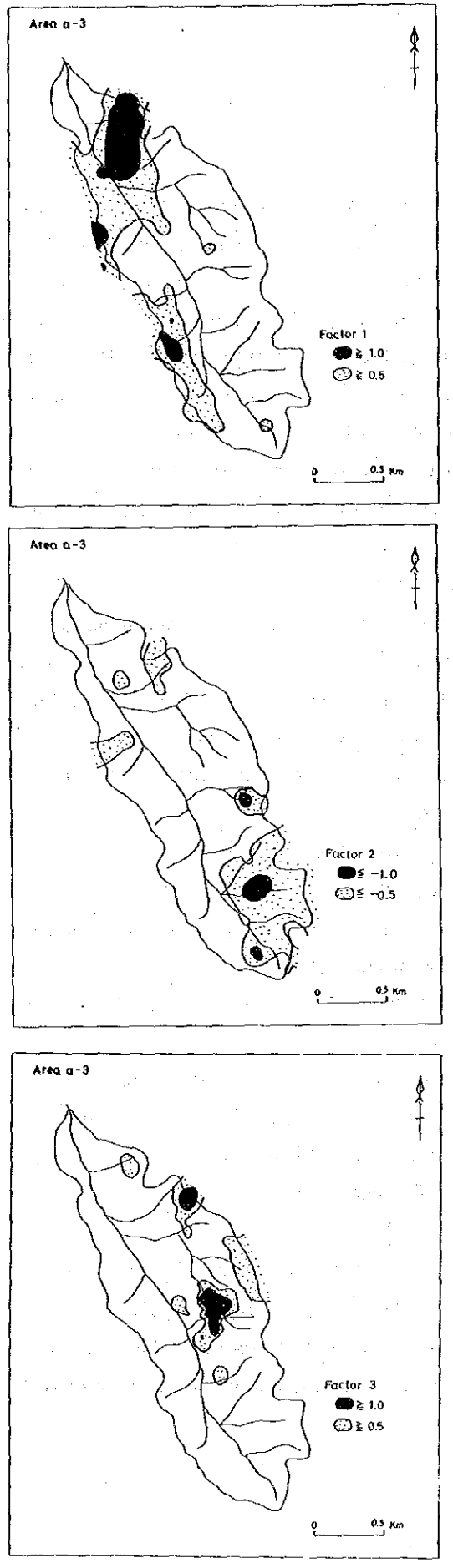

Fig. II - 4 - 5 Factor analysis map in the Area a-3

Due to poor exposures, the relationship between Factor 2 and geology were not so clear.

Factoe 3 (Sn, (As), (Cu))

Among Factor 3 elements, Sn and As present large positive values but Cu presents a large negative value.

The Factor 3 score map shows large positive scores as high scores. High score zones are distributed on a small scale in the central and northern parts of the area. Their configurations are same as those of Sn anomalies in the EDA interpretation map.

4-2-2 Discussion

The geochemical anomalous zone of each element obtained in the area tends to extend along a NNW - SSE direction, which coincides with a direction of S. Chebor (may be tectonic valley) and with the schistosity of phyllite.

Though granite is not exposed in and around the area, it is conceivable that Au, Sn and As mineralization were accompanied by subsurface granite intrusion along S. Chebor tectonic zone.

4-3 General Discussion on the Survey Results

Near the boundary between the Main Range granite and phyllite, tin deposits are expected. Actually 4 mines are operating on the north bank of S. Bidor. Occurrence of the deposits are lenticular cassiterite - quartz veins which is parallel to the schistosity of phyllite while cassiterite - tourmaline - quartz veins which are perpendicular to the former.

The area a-3, located 1km west of the Main Range granite, is entirely composed of phyllite. One old mine workings was found in this phase, seeming the same type of tin mineralization.

Geochemical soil survey disclosed an Au anomalous zone on the eastern side of S. Chebor, which runs in the center of the area.

The anomalous zone includes the old mine workings and extends in a NNW - SSE direction. On the eastern side of the zone Sn anomalies are scattered. Other Au anomalous zones spread towards the watershed on the western side of S. Chebor. These anomalous zones are probably merged to only one under Quaternary sediment which is distributed along S. Chebor.

Cu anomaly zones are distributed on the western side of S. Chebor and none, on the eastern side.

Based on the evidences (1) S. Chebor runs almost rectilinearly, (2) the eastern side of S. Chebor differs in topography from the western side, and (3) Cu anomalous zones occur only on the west side of S. Chebor and their boundaries stretch rectinearly along the river.

It can be presumed that S. Chebor is a tectonic valley and that mineralization took place along this valley. However, the low values of anomalies of Au (mean = 0.095ppm, maximum = 0.135ppm) suggest low potential for Au resources in this area.

PART III AREA B

Chapter 1 Outline of the Area b Survey

1-1 Outline of the Survey

The Quaternary Formations extending from Tapah to Teluk Intan has been investigated by GSM. From 1982, 175 shallow boreholes and 22 deep boreholes were drilled.

Each hole encountered clay, silt, sand, gravel and peat of netric estuarine deposits. In the Labu Kubung area to the northeast of Teluk Intan, placer tin minerals are concentrated in sand and gravel beds on or near the bedrock of Paleozoic at the depth of 70-80m from the surface.

According to GSM data, this tin concentration was confirmed by six boreholes, showing an area of 3km x 8km with 1.5 - 6.0m in thickness and 0.24 - 1.29kg/m^3 in SnO_2 content.

As the thickness of the beds is considered to be affected by the bedrock topography, a detailed gravimetric survey was carried out in the most promissing area (30 km^2) in order to estimate depth of the bedrock. In parallel to the survey, 3 boreholes were drilled to check applicability of gravity method through comparison between estimated depth and drilled depth.

1-2 Objectives of the Survey

The objectives of the survey for the Area B are to clarify the bedrock relief (through gravity survey) which seems to control the distribution of placer tin deposits, to clarify the details of placer tin deposits and clay beds (through drilling) and to check applicability of gravity survey through comparing the results of the survey and the drilling.

1-3 Amount of the Survey

The amount of survey carried out in Area b in this phase is shown in Table III-1-1.

Table Ⅲ-1-1 Amount of survey in the Area b

Method	Amount	
Geophysical survey (Gravimetric)	Survey area	30㎢
	Measuring points	860points
Drilling	Total drilling length	237.3 m
	MJMP-1	98.0 m
	MJMP-2	76.5 m
	MJMP-3	62.8 m

2-1 Method of Survey

2-1-1 Introduction

The earth's gravity is a composite force which combines mainly the attraction due to the earth's mass and the centrifugal force caused by the earth's rotation. Gravity becomes maximum on the poles and minimum on the equator. A body on the surface of the earth has a 'weight' which results from the gravitational attraction between the body and the entire earth's mass. The unit of acceleration is the gal, named after Galileo (1 gal=1cm/sec^2). The average acceleration on the earth's surface is about 980 cm/sec^2=980 gals. Gravitational anomalies are only very small fractions of the earth's field, so a smaller unit is needed. The unit commonly used in gravity survey is the milligal or mgal which is equivalent to 0.001 gal. Anomalies from local geologic structure are commonly in the order of several milligals.

Gravity value (g) on the earth's surface is given by the following formula;

$$g = GM/R^2 - \omega^2 R\cos\phi$$

where,

M	:	Mass of the earth
G	:	Gravity constant
R	:	Radius of the earth
ω	:	Angular velocity
ϕ	:	Latitude

The shape of the earth could be assumed as an ellipsoid of revolution. Thus, a gravity value on the ellipsoid is regarded as a value on the earth's surface. A standard gravity value on the earth is given by the next formula recommended by International Union of Geodesy and Geophysics (IUGG). IUGG adopted in 1971 the International Gravity Standard Network (IGSN).

$$\gamma_{1967} = 978.03185(1 + 0.005278895 \cdot \sin^2\phi - 0.000023462 \cdot \sin^4\phi) \ \lceil gal \rfloor$$

IUGG recommended in 1980 an updated gravity formula. The formula is as follows.

$$\gamma = \frac{a\gamma_e \cos^2\phi + b\gamma_p \sin^2\phi}{\sqrt{a^2\cos^2\phi + b^2\sin^2\phi}} \ \lceil gal \rfloor$$

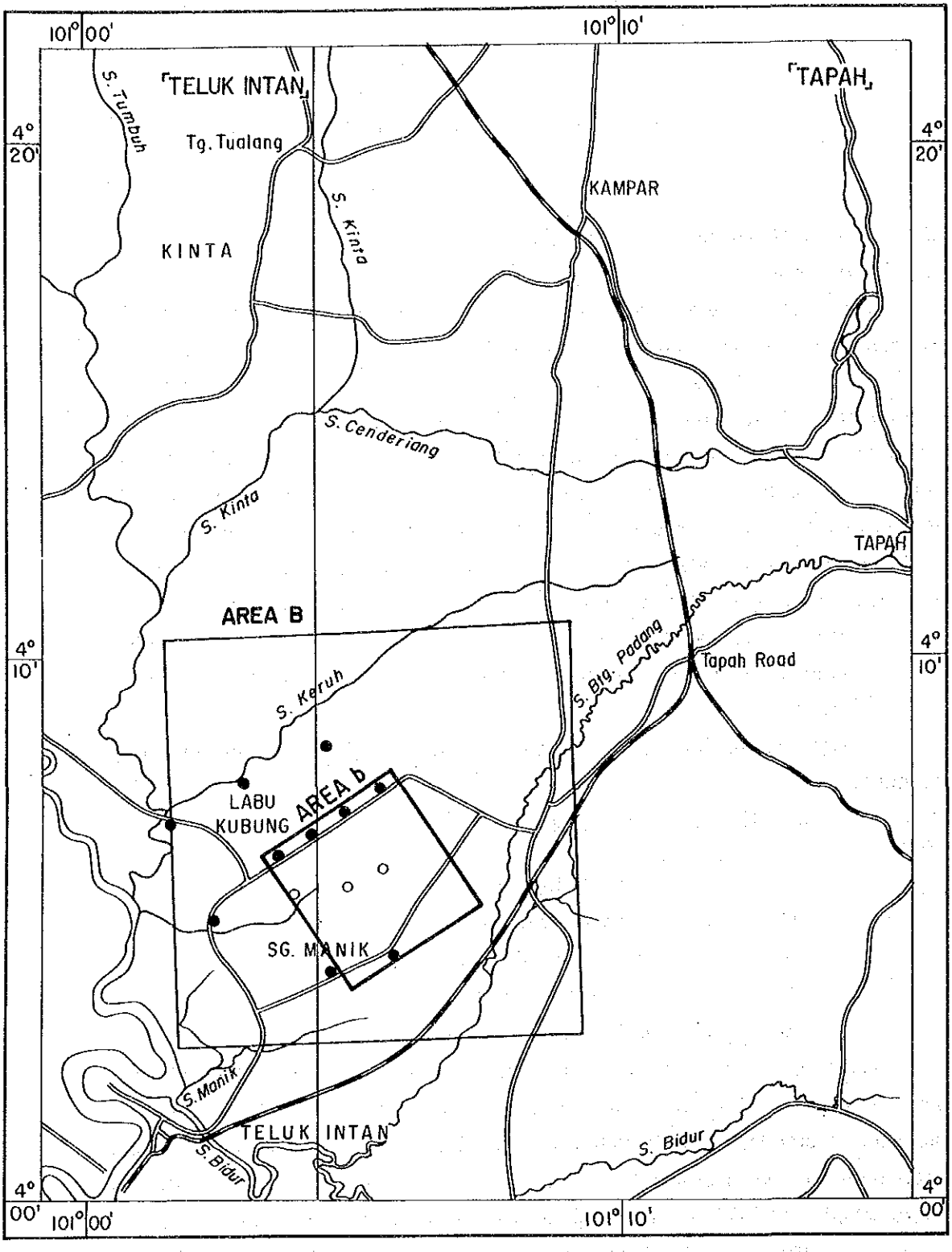

Fig. III - 2 - 1 Location map of the geophysical survey area

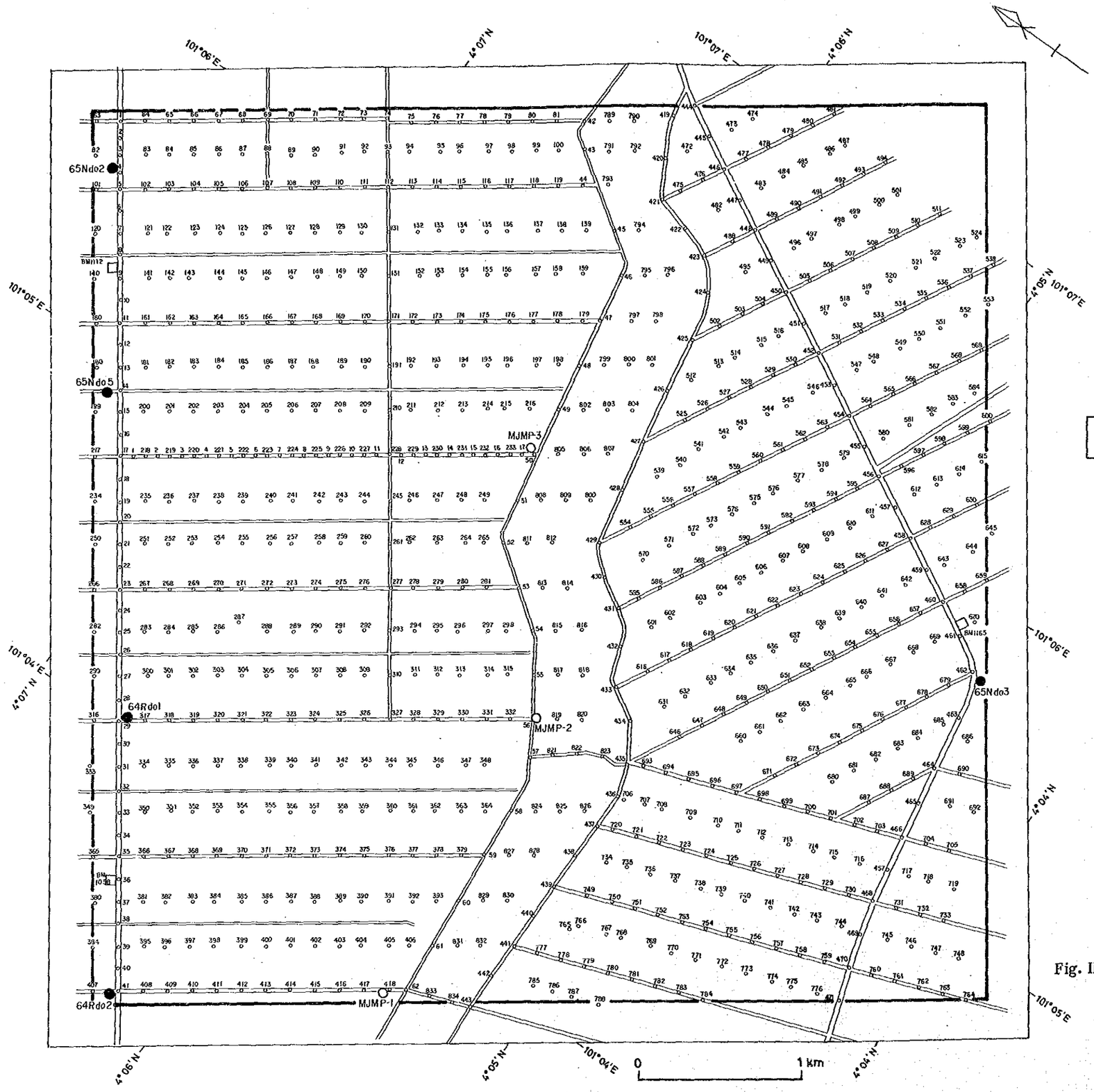

Fig. III - 2 - 2 Location map of the measured gravity points

$$\gamma_{1980} = 978.03267715\ (1 + 0.052790414 \cdot \sin^2\phi + 0.0000232718 \cdot \sin^4\phi + 0.0000001262 \cdot \sin^6\phi + 0.0000000007 \cdot \sin^8\phi)\ \text{[gal]}$$

2-1-2 Survey Planning

Observation points are shown on the location map of Fig. III-2-2. Planned points were 800 points, however, actual observation points resulted in 860. In order to detect a detailed basement structure, 60 points were added on the road connecting with previous drilling holes. All the points were measured by leveling. With the exception of the gravity station No.1000, the points measured were numbered from 1 to 834 sequentially. Other additional points on the road connected with drilling holes between 64Rd01 and MJMP-2, were numbered from 901 to 917, at MMAJ drilling holes from 951 to 953, and at GSM drilling holes from 961 to 966. The survey area was about $5km^2$, and the standard interval between points was 150m. The observation points were densely distributed on the roads as well as on footpaths in the survey area. To increase accuracy, the points were located by using a pocket compass to connect them.

2-1-3 Gravity Meter

La Coste G type gravity meter was used. Specifications are as follows.

Table III-2-1 Specifications of the gravity meter used

No. of Production	G-236
Operating range (mgal)	0-7440.76
Temperature of heater (°C)	47.5
Reading line	2.60

La Coste gravity meter is characterized by its worldwide range without the need of resetting. Its negligible drift is normally less than 0.5 mgal/month.

2-1-4 Standard Gravity Value

In peninsula Malaysia, IGSN (International Gravity Standardized Net) stations have been established. Gravity base station (No.1000) was set at the entrance of a rest house in Teluk Intan city, located at 20km southward from the survey area with a IGSN station in Tapah city. Table III-2-2 shows gravity values at the gravity base stations.

Table III-2-2 Gravity standard value

Base station	Location		Gravity value (mgal)
	Latitude (Deg., Min., Sec.)	Longitude (Deg., Min., Sec.)	
TAPAH	4°12'00"	101°15'30"	978025.765
T. INTAN (No.1000)	4°01'15"	101°01'20"	978078.334

2-1-5 Leveling

The direct leveling method was adopted for all points by using the Auto Level B-2 of Sokkisha, Japan. Some bench marks for leveling were adopted by using three known elevation points along the route 70 across the survey area. Location of Bench marks are as follows;

Elevation of Bench Mark

Bench mark	Elevation(m)	Location	
		Latitude	Longitude
BM1058	4.054	04°06'24"	101°03'34"
BM1112	9.613	04°07'25"	101°05'03"
BM1165	5.957	04°04'33"	101°05'54"

Leveling was carried out by setting closed traverses as possible to increase accuracy. Closure error of leveling routes are shown in Table III-2-3.

Table Ⅲ-2-3 List of leveling error

Order	Route	Observed elevation difference (m)	Closed Error (mm)	Distance of closed loop (D, km)	Precision required (mm)
1	BM1112-10-20-BM1058	-5.571	+12	3.8	$6\sqrt{D}$
1	BM1112-80-50-60-41-BM-1058	-5.570	+11	12.2	$3\sqrt{D}$
1	435-441-470-BM1165-444-435	-0.019	-19	14.1	$5\sqrt{D}$

2-1-6 Gravity Calculation and Corrections

Flow chart of gravity calculation and corrections is shown in Fig. III-2-3.

(1) Gravity Calculation

1) Conversion

To obtain the gravity value in milligals from the reading of the counter and dial of the gravity meter, conversion values of the gravity meter are employed. These conversion values are given for every 100 units interval of the counter. Gravity values in milligals are obtained by the next formula;

$$V\gamma_k = K_{100} + (123.456 - 100.000) \times k_{100}$$

Vr_k : Observed gravity value
Vr : Reading indicated by the counter
Vro : Reading for each 100 units interval of the counter
K_{100} : Gravity meter constant
K_{100} : Conversion factor

2) Tidal Correction

Tidal forces are due to the attraction of celestial bodies such as the sun and the moon at the earth's surface. They deviate in direction and intensity depending on the observed time and place of observation.

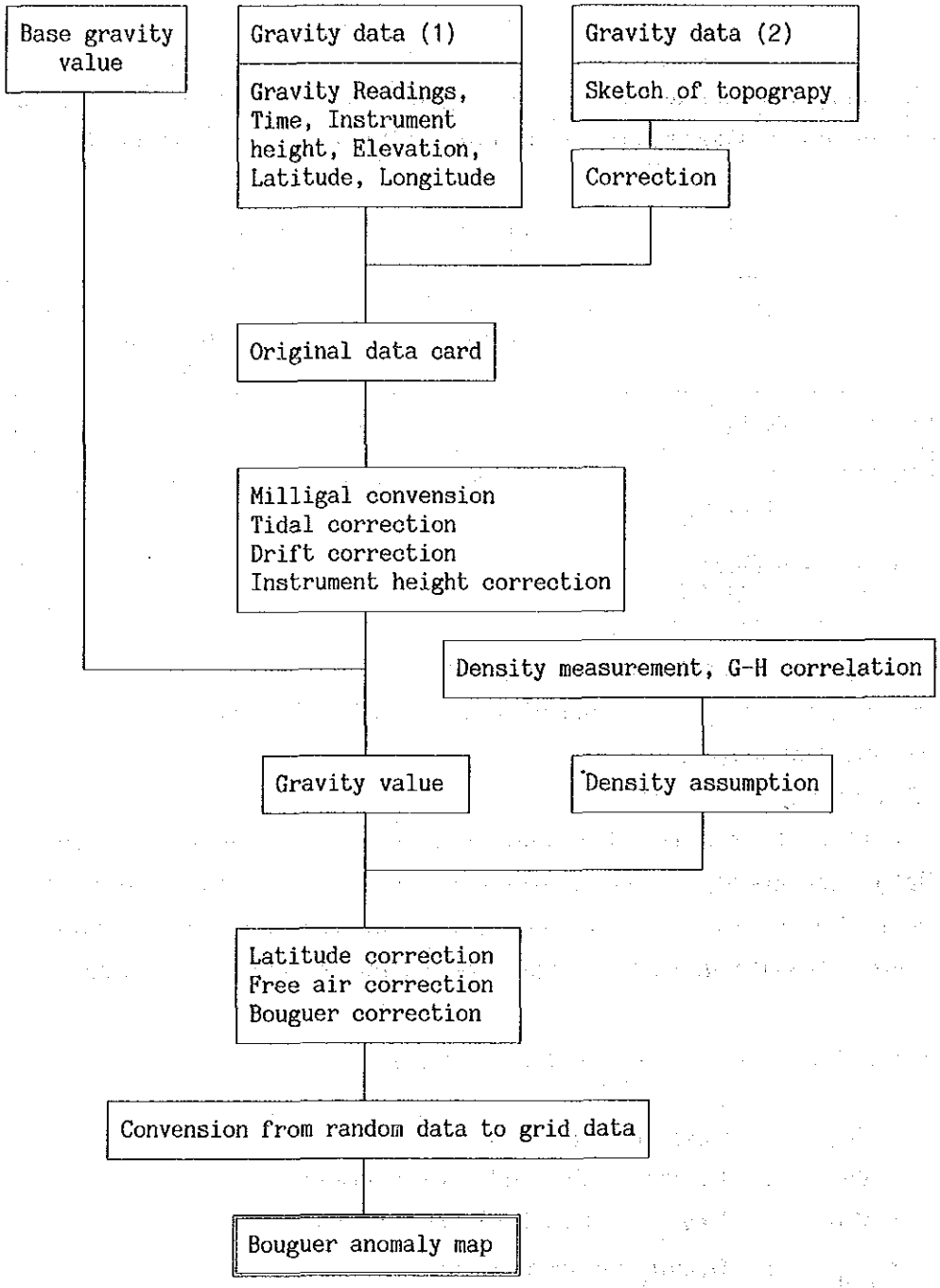

Fig. Ⅲ-2-3 Flow chart of the gravity analysis and interpretation

Tidal force due to the sun and the moon is calculated by the following formula;

$$Vet = -\Sigma\ 1.16\ u$$

$$u = -\frac{3}{2} \cdot G \cdot M \cdot \frac{a}{r^3} \left\{3\ \left(\sin^2\delta - \frac{1}{3}\right) \cdot \left(\sin^2\phi - \frac{1}{3}\right) + \sin 2\delta \cdot \sin 2\phi \cdot \cos^2\theta + \cos\delta \cdot \cos^2\phi \cdot \cos 2\theta\right\}$$

where,

Vet	:	Tidal correction values
u	:	Tidal force due to the celestial body
G	:	Gravitational constant
M	:	Mass of the celestial body
a	:	Distance from center of earth to observation point
r	:	Distance between the earth and the celestial body
δ	:	Declination of the celestial body (angle from the equator to south or north)
ϕ	:	Latitude at observation point
θ	:	Angle of the celestial body (Angle between terrestrial and planetary meridian plane)

In order to check the tidal correction parameter, gravity observations at a gravity base station were made. Two peaks and three bottoms were observed for 29 hours from 7:30 a.m. on Aug. 26 to 15:00 p.m. on Aug. 27 at the entrance of the rest house in Teluk Intan city.

Good agreement were found between values observed and values calculated. The error is only less than ten or more micro gals. Thus, a tidal constant of 1.16 was adopted. The observed results are shown in Fig. III-2-4.

3) Instrument Height Correction

This correction is used to adjust the instrument height from the elevation of the point on the ground determined by leveling.

Vhi=0.3086 hi x 100

where,

Vhi	:	Correction of instrument height
hi	:	Height from the ground to the top of gravity meter (cm)

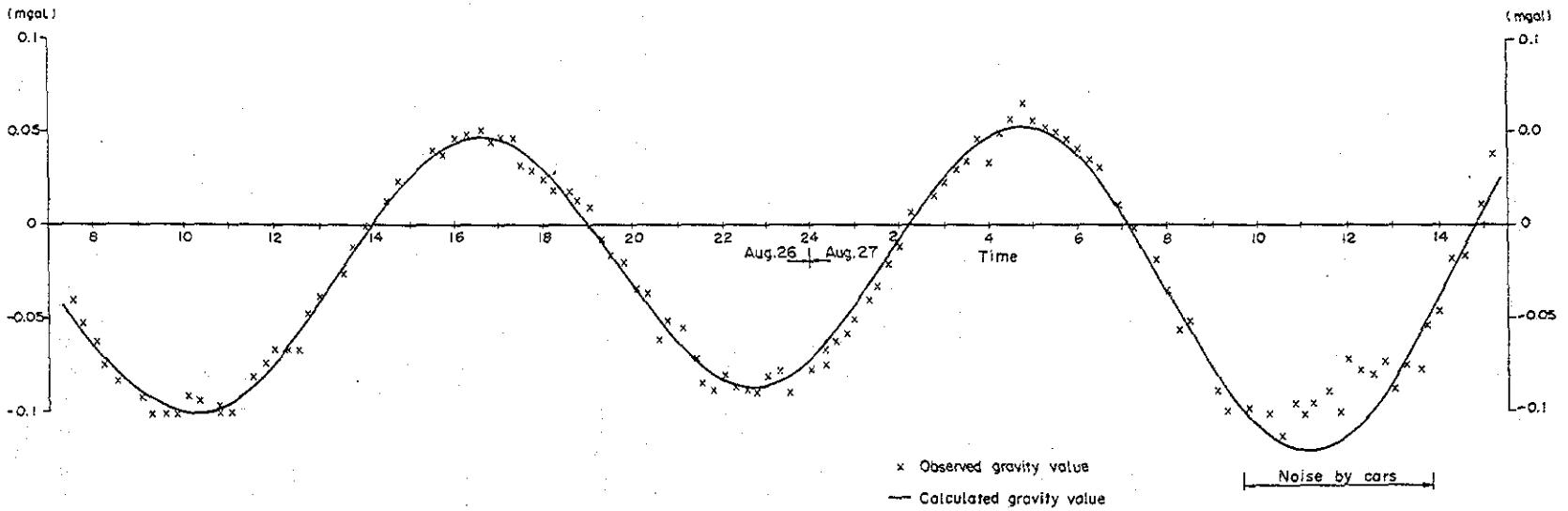

Fig. III - 2 - 4 Gravity measurement to estimate the tidal constant at station

4) Drift Correction

Drift is an inherent error of a gravity meter which changes proportionally with time. In the survey, the closure error was regarded as a drift and distributed by the corresponding time interval.

5) Gravity Value

Corrections on the observed value are as follows;

$$g=(Vrk+Vhi+Vd-Vg)+Bg$$

where,

g	:	Gravity value at an observation point
Vc	:	Corrected gravity value
Vrk	:	Observed gravity value
Vhi	:	Instrument correction value
Vd	:	Drift correction value
Vg	:	Corrected gravity value at a gravity base point
Bg	:	Gravity value at a gravity base point

(2) Gravity Correction

A flow chart of various corrections from a gravity meter reading to its corresponding Bouguer anomaly value is shown in Fig. III-2-3.

1) Free Air Correction

This is a required correction for the elevation of a gravity point because the measurement is made at a different distance from the center of the earth. Free air correction can be got by the next formula;

$$\delta g o = \alpha \cdot Hm$$

where,

$\delta g o$: Free air correction value

Hm : Elevation at a gravity point

α : Free air constant (mgal/m)

[*1] From Hagiwara (1982), free air constant is variable from the equator to the pole of the earth. It is -0.3083 in the polar area, -0.3086 in the middle, and -0.3088 in the equator area. A free air constant of -0.30878 was adopted in this survey.

2) Terrain Correction

A topographic irregularity (hill, slope, ditch etc.) will exert an attraction directly proportional to its density. The vertical component of this attraction will be directed upwards and this reduces the gravity value.

A term of this magnitude must therefore be added to the measured value of gravity. A gravity point near a valley is a negative mass and the vertical component of its attraction will also be directed upwards leading again to an additive topographic correction. Generally, terrain correction needs to be adopted up to about 60km from the gravity point. In the survey, however, topography is flat, and the survey area is located 20km far from the mountainous area. Therefore, since terrain correction values were negligible less than several tens micro gals, a terrain correction within only 20m (close) from a gravity point was adopted to remove the effect of patches. This close correction is made within 20m from the corresponding gravity point.

* Close Terrain Correction

The nearest topography within 20m from the gravity meter is sketched and a 2-dimensional topographic section is simply modified as mentioned below. The correction due to the close cliff, slope and channel are calculated as,

$$\delta g_0' = 2G\rho \int_0^R \left\{ \tanh^{-1} \sqrt{\frac{R^2-X^2}{R^2+H_0^2}} - \tanh^{-1} \sqrt{\frac{R^2-X^2}{R^2+(X\tan\beta+H-H_0-D\tan\beta)^2}} \right\} dX$$

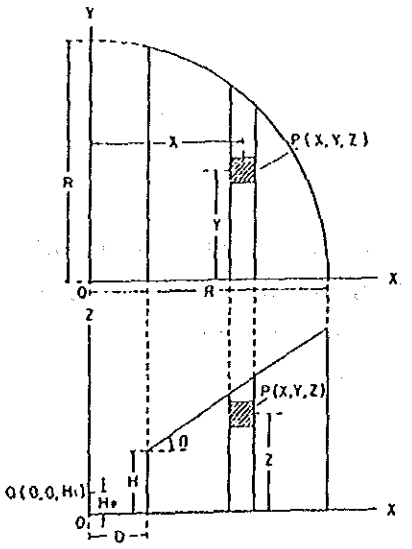

$\delta g_0'$	:	Terrain correction value
G	:	Gravity constant
ρ	:	Density (1.8 g/cm^3)
D	:	Distance from a gravity point to cliff
H	:	Height of cliff
β	:	Angle of cliff
R	:	Extension of the correction area
H_0	:	Height of the center of the gravity meter (0.15m)

3) Bouguer Correction

Bouguer correction is a height correction caused by the attraction of the rock mass between the individual station and the mean sea level or by the absent of mass between them. Bouguer correction value is given as follows;

$$\delta g_0'' = -2\pi G \rho Hm = -0.0419 \rho Hm$$

Hm : Altitude in meter at the gravity point

ρ : Density of the intervening rock between surface and the mean sea level

4) Latitude Correction

The attraction of gravity on the earth decreases towards the equator and increase towards poles because of the centrifugal force resulting from the earth's rotation and of the earth's radius due to polar flattening. Latitude correction is the difference value between theoretical and observed. Theoretical value can be given by the Normal gravity formula recommended by IUGG (International Union of Geodesy and Geophysics) in 1967.

In the survey, the following formula was used for the calculation of the standard gravity value;

$$\gamma_{1967} = \frac{a\,\gamma_E \cos^2\phi + b\,\gamma_P \sin^2\phi}{\sqrt{a^2\cos^2\phi + b^2\sin^2\phi}}$$

γ_{1967} : Normal gravity value

a : Radius of the earth at the equator (6,378.140km)

b : Radius of the earth at the polar (6,356.775km)

γ_E : Standard gravity value at the equator (978.03184558 gal)

γ_P : Standard gravity value at the polar (983.21772792 gal)

ϕ : Latitude

A simplified formula of the above and useful for the survey purposes, is shown as follows;

$$\gamma_{1967} = 978.0318\ (1 + 0.005278895 \sin^2\phi - 0.000023462 \sin^4\phi)\ \text{[gal]}$$

γ_{1967} : Standard gravity value

ϕ : Latitude

5) Bouguer Anomaly

The difference value between the corrected gravity resulting from the above mentioned corrections and the standard gravity is called Bouguer anomaly.

$$\Delta g o'' = g + \delta g o + \delta g o' + \delta g o'' - \gamma_{1967}$$

$\Delta g o''$: Bouguer anomaly value

The Bouguer anomaly varies according to the densities assumed. Three Bouguer anomaly maps have been made (assumed densities were 1.6, 1.8 and 2.0 g/cm^3) in the survey.

2-1-8 Assumption of Density

To analyze underground structure by the gravity method in the survey area, it is necessary to prepare a Bouguer anomaly map by an assumed density most suitable for the area. In the survey area, two methods were used: measuring the density of rock samples and using a G-H correlation chart to determine an optimum assumed density. Consequently, ρ=1.8 g/cm^3 was decided as the optimum assumed density there.

1) Measurement of Density of Rock Samples

The geology of the survey area consists of two layers: a quaternary formation and a Paleozoic formation with intrusive of Paleozoic Granites.

Generally, assumed density is for formations up to 0 m above sea level. So, in this survery area the density of the quaternary formation had to be used. But samples for density measurement could not be taken there because of low concretion of the local quaternary formation. Therefore, 1.8 g/cm^3, the mean value of density of sand in general (1.4-2.2 g/cm^3), was used in this survey.

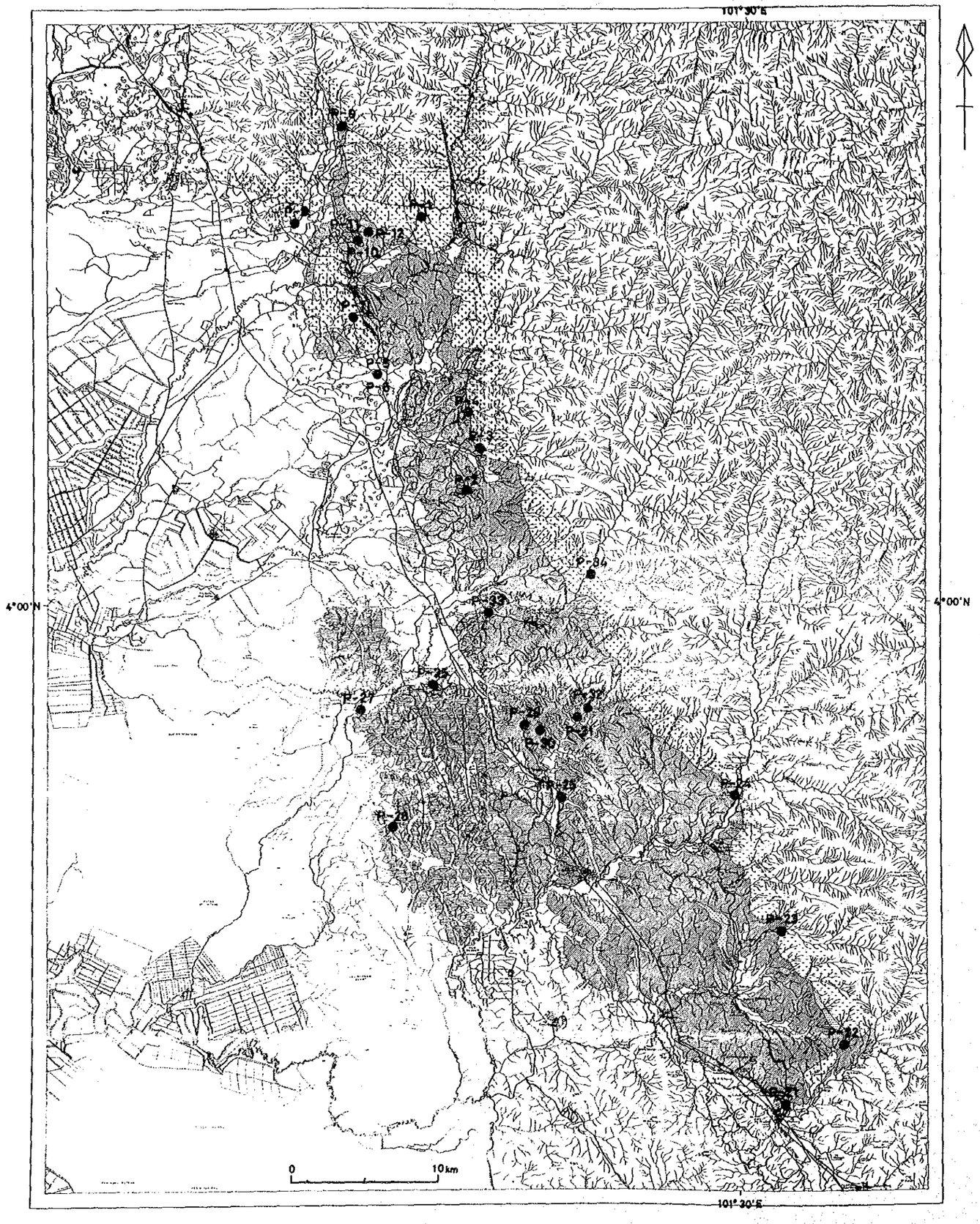

LEGEND

- Quaternary Formation — Clay, sand, gravel
- Belata Formation — Phyllite; Metasandstone
- Terolak Formation — Green Schist; Phyllite; Metasandstone, psammitic schist

(Intrusive Rocks)

- Main Range Granite — Porphyritic granite; Equigranular granite; Granite porphyry
- Changkat Rambian Granite — Equigranular granite
- Mineral showing (Major quartz vein)
- Kaolinization
- 40 — Dip and strike of schistosity
- Geological boundary
- Inferred fault
- Anticline
- Syncline
- Lineament extracted from aerial photographs
- Sampling point

Fig. III - 2 - 5 Location map of the rock samples collected

In the survery area, 24 pieces of rocks, believed to come from the basement (granite, schist, etc.), were taken from drill holes and outside the survey area and their densities were measured in three states: dry, natural and wet to presume basement structures. The measurements are listed in Table III-2-4 while Fig. III-2-5 shows the location from which the samples were taken. Table III-2-5 consolidates mean densities by types of rocks and distribution of densities.

2) G-H Correlations

A gravity value decreases as the measured point elevation increases. The decrease rate is equal to the sum of free air and Bouguer correction (0.3086-0.0419 ρ)/m. So, if a gravity value with a corrected latitude is plotted, using the measured point elevation as the axis of abscissas and the gravity value as the axis of ordinates, the average rock density in the survey area can be presumed from the slope of the straightline formed by the points.

The G-H correlation chart in Fig. III-2-6 expressed the correlations between the measured point elevation and the gravity value. The density determined by this correlation chart is -19.62. This value is clearly anomalous since densities determined by this method normally ranges roughly from 1 to 3. Therefore, the density thus determined is considered to be inappropriate to this survey area. The presumed reasons for this include (1) small elevation differences (maximum 12 m) and (2) regional gravity trends.

2-2 Method of Analysis

The analysis was made according to the flow chart shown in Fig. III-2-7.

The gravity anomalies were observed on the ground surface. The gravity differences reflected the undreground structures with different depths and different shapes. So, it is necessary to make the analysis that can express the target ground structure accurately and easily. Therefore, anomalies must be analyzed by carrying out filter treatment for the Bouguer anomaly map with a suitable assumed density. In the survey, analysis was

Table. Ⅲ-2-4 List of rock densities

SNo.	Sample No.	Rock name	Density (g/cm³)			Porosity (%)
			Natural	Wet	Dry	
1	P-1	Granite	2.66	2.66	2.66	0.77
2	P-2	Phyllite	2.37	2.37	2.16	20.78
3	P-3	Schist	2.64	2.65	2.61	4.48
4	P-4	Granite	2.66	2.66	2.65	0.66
5	P-5	Clay	1.53	1.58	0.95	62.79
6	P-6	Silt	1.42	1.55	0.92	62.61
7	P-7	Granite	2.54	2.56	2.49	6.61
8	P-8	Granite	2.63	2.63	2.59	4.28
9	P-9	Granite	2.62	2.63	2.62	1.32
10	P-10	Phyllite	2.26	2.27	2.02	25.08
11	P-11	Phyllite	2.49	2.50	2.34	15.30
12	P-12	Horanfels	3.04	3.04	3.04	0.16
13	P-21	Slate	1.68	1.85	1.44	40.06
14	P-22	Slate	2.54	2.54	2.49	5.59
15	P-23	Granite	2.63	2.63	2.62	0.88
16	P-24	Granite	2.67	2.67	2.66	0.88
17	P-25	Phyllite	2.43	2.45	2.28	17.48
18	P-26	Phyllite	2.34	2.37	2.15	22.17
19	P-27	Sandstone	2.40	2.42	2.28	13.79
20	P-28	Sandstone	2.50	2.51	2.43	8.81
21	P-29	Phyllite	1.50	1.75	1.28	47.27
22	P-30	Schist	2.25	2.32	2.14	17.54
23	P-31	Sandstone	2.47	2.49	2.38	10.26
24	P-32	Granite	2.45	2.46	2.36	9.79
25	P-33	Phyllite	2.40	2.42	2.33	9.07
26	P-34	Granite	2.57	2.58	2.55	2.83

Table. Ⅲ-2-5 Average of classified rock densities

Periods	Rock name	Number of samples	Average (g/cm³)		Density (g/cm³) 2.0 2.5
Quarternary	Silt, clay	2	1.57		–
Paleozoic	Granite	9	2.61	2.55	—
	Phyllite	6	2.31		—
	Schist	2	2.65		—
	Slate	2	2.54		• •
	Sandstone	3	2.47		—

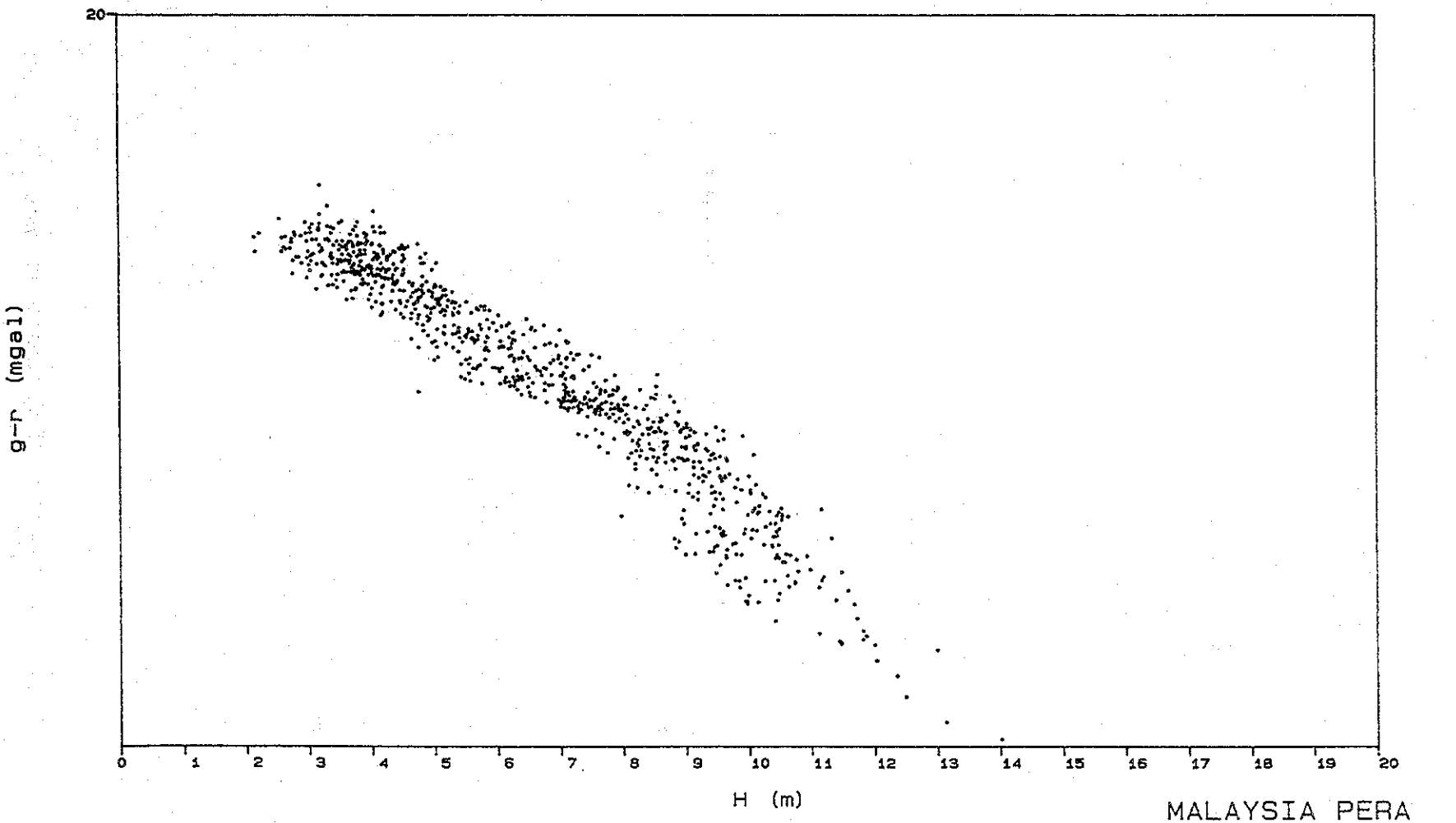

Fig. III - 2 - 6 G-H correlation

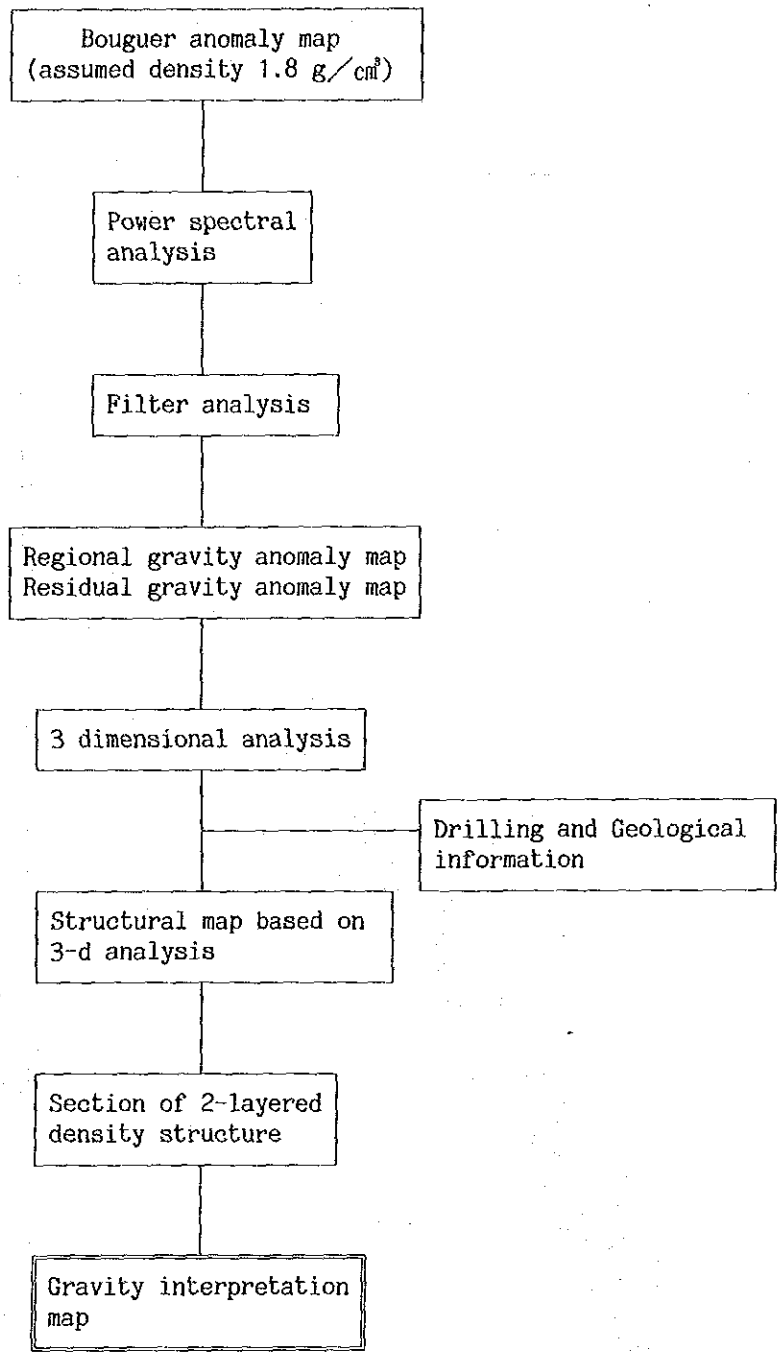

Fig. Ⅲ-2-7 Flow chart of the gravity analysis

conducted after classifying wavelengths into long wavelengths reflecting a regional trend and short wavelengths reflecting the object basement structure. The treatment of the data was made according to the flow chart in Fig. III-2-7.

2-2-1 Filtering

As stated above, gravity anomalies observed on the ground surface are the gravity variations due to different depths and shapes. So, it was conducted the power spectral analysis of Bouguer anomalies and separeted frequency bands by the results of the analysis. For the analysis, the fast Fourier Transform (FFT) method with a high computing accuracy was used. A total of 1089 gridded data: 33 along the Y (northeastern) direction by 33 along the X (southwestern) direction with grid intervals of 170 m was used for the analysis.

(1) Power Spectral Analysis

This analysis was conducted using a power spectral analysis chart prepared to presume mean depths and wavelengths on underground density boundaries. The power spectral analysis chart was prepared by performing Fourier Transform analysis for the gravity distribution g(x, y) of the plane and computing the power spectrum (Pmn). The mean depth (Do) of the boundary of each layer can be presumed and the filtering wavelength of each layer can be obtained from the slope of this power spectrum distribution.

$$\ln P_{mn} = C - 4\pi D_o \left\{\sqrt{(m/N_x)^2 + (n/N_y)^2}\right\}$$

C : Constant concerning density

Nx, Ny : Number of survey points in x and y directions

m, n : Wave number in x and y directions

(2) Filtering

The Bouguer anomaly map was separated into three wavelength bands (noise, residual and regional) by high-cut filtering using the band separating wavelength obtained from the power spectral analysis. Supposing that the Fourier Transform of the gravity potential G (x, y) is F (u, v), the computation of the high-cup filter can be indicated by the following expression;

$$G\lambda(x, y) \equiv F(u, v) \cdot \exp(-\lambda(u^2+v^2))$$

Here, is the coefficient to be determined by the wavelength to be high-cut.

2-2-2 3-Dimensional Structural Analysis

There are innumerable solutions to give a certain potential distribution a potential distribution that is identical to it. Of these, the solution that suits the local geological structure best is adopted.

For gravity distribution, various assumptions are made including the followings;

(1) That the underground structure causing this gravity anomaly is the sedimentary structure of which the underground density change is function of the depth.

(2) That it is a two-layer structure composed of a sedimentary layer with uniform density and a base rock.

It is common practice to analyze so as to correspond to the geological structure in the survey area for the residual gravity anomaly obtained by filtering. In this analysis, the method of analyzing the frequency domain and for computation by the fast Fourier Transform (FFT) was used.

In the analysis of frequency domains, the underground density distribution is presumed from the gravity distribution transformed into a frequency domain. First, supposing that the Fourier transform of the gravity distribution g(x) is $F(\omega)$, $F(\omega)$, gravity distribution at the mean depth D of the underground structure can be indicated with $\exp(\omega D)\ F(\omega)$ by downward continuation. This is equivalent to the gravity by condensation density $\rho^*(\omega)$ at the depth D. The distribution of these condensation densities can be substituted by $\rho^*(\omega) = \Delta\rho \cdot H(\omega)$ if the density difference between the two layers is and if the amplitude change in the density distribution at the mean depth D is H (a).

It is, therefore, possible to find H(w) from

$$\exp(\omega D)\ F(\omega) = 2\ G\ \Delta\rho\ H(\omega)$$

and find the depth change h(x) on the boundary in the two-layer structure from this inverse Fourier transform. In other words, depth distribution in a two-layer structure can be determined by S(x)=D-h(x). Here, G is the gravity constant, is a variable after Fourier transformation and x is a variable.

In this analysis, corrective computation repeatedly was made, by using confirmed basement depths in eight drill holes in the survey area as control points and changing the combination of mean depth D and density difference so as to agree with each depth. The density difference and mean depth used in the computation were determined by referring to density sample measurement data and drilling data. The section analysis shows the results of a three-dimensional structural analysis.

2-3 Results of Analysis

2-3-1 Bouguer Anomaly Map

As stated in 2-1-8, the Bouguer anomaly map with an assumed density of ρ =1.8 g/cm^3 (Fig. III-2-9) was selected for this survey area. Bouguer anomaly maps with two assumed densities (1.6 g/cm^3 and 2.0 g/cm^3) (Fig. III-2-8 and Fig. III-2-10) are also attached to the report. The characteristics of the Bouguer anomaly map (assumed density: 1.8 g/cm^3) for this area are described below.

The Bouguer anomaly values in the survey area are within the range of 7 mgal to 15 mgal and tend to increase gradually from the northeastern part of the area to the southwestern part. The trend of gravity contour lines prevails in the NW-SE direction. Particularly, a gravity high gradient zone showed a fault that can be clearly seen at the northeastern end of the area.

The central part of the area presents a high/low gravity anomaly with a great wavelength (half-wave length: about 1 km) which reflects the structure of the basement. It is presumed that the high gravity anomaly is an anomaly corresponding to a crest in the basement while the low gravity anomaly on the west side of the high gravity anomaly is an anomaly corresponding to a hollow in the basement.

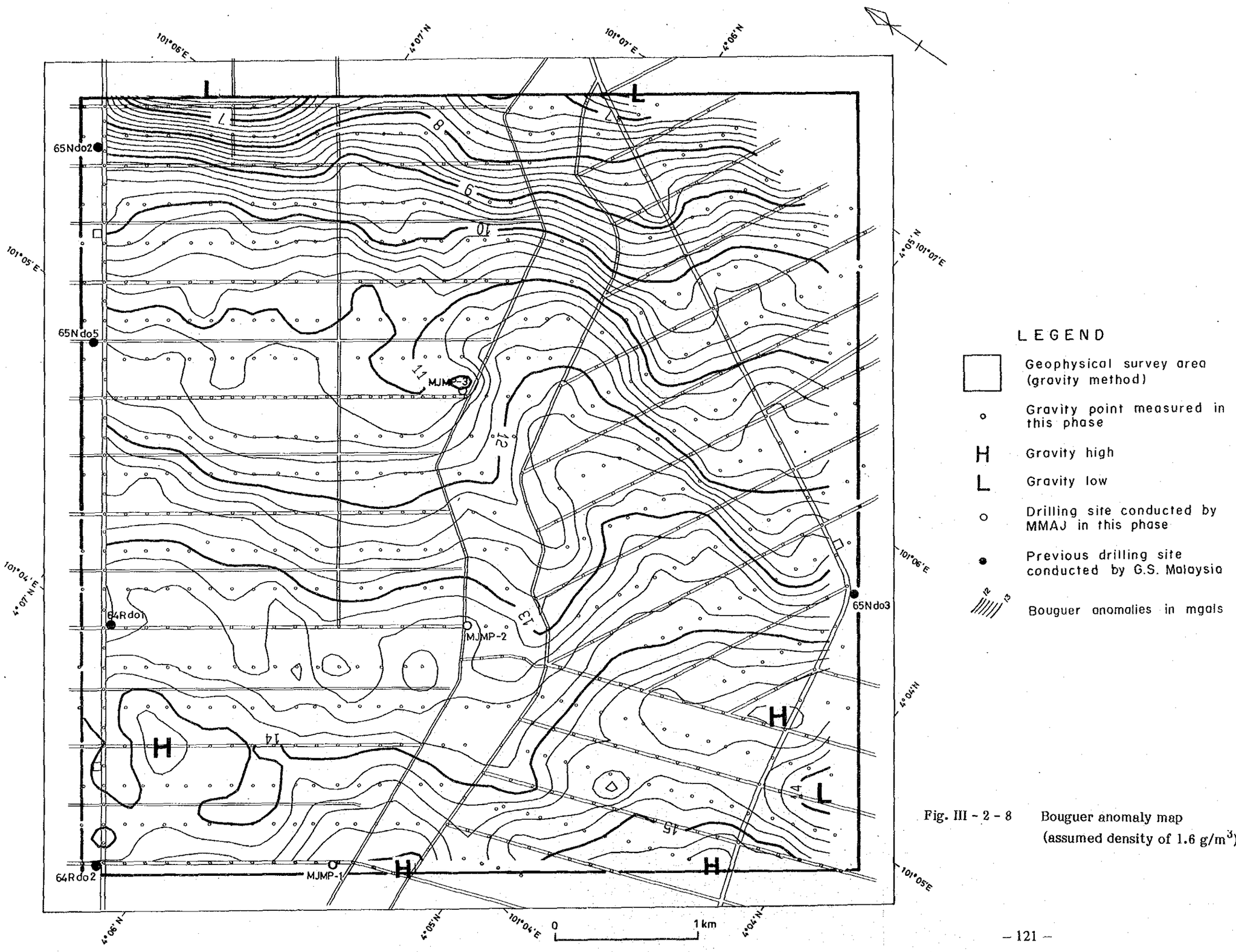

Fig. III - 2 - 8 Bouguer anomaly map (assumed density of 1.6 g/m^3)

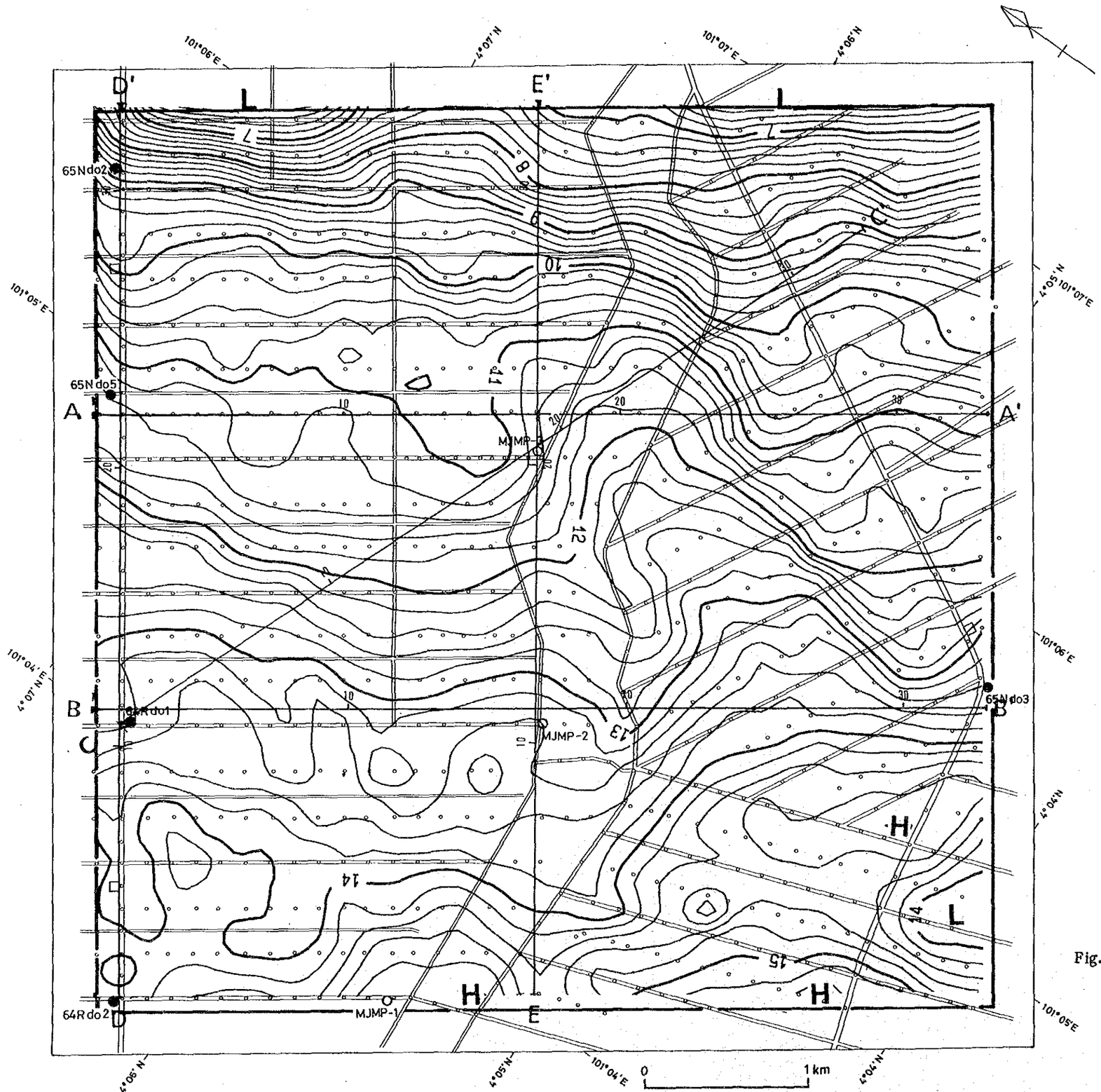

LEGEND

- Geophysical survey area (gravity method)
- Gravity point measured in this phase
- H Gravity high
- L Gravity low
- B—B' Section line
- Drilling site conducted by MMAJ in this phase
- Previous drilling site conducted by G.S. Malaysia
- Bouguer anomalies in mgals

Fig. III - 2 - 9 Bouguer anomaly map (assumend density of 1.8 g/m^3)

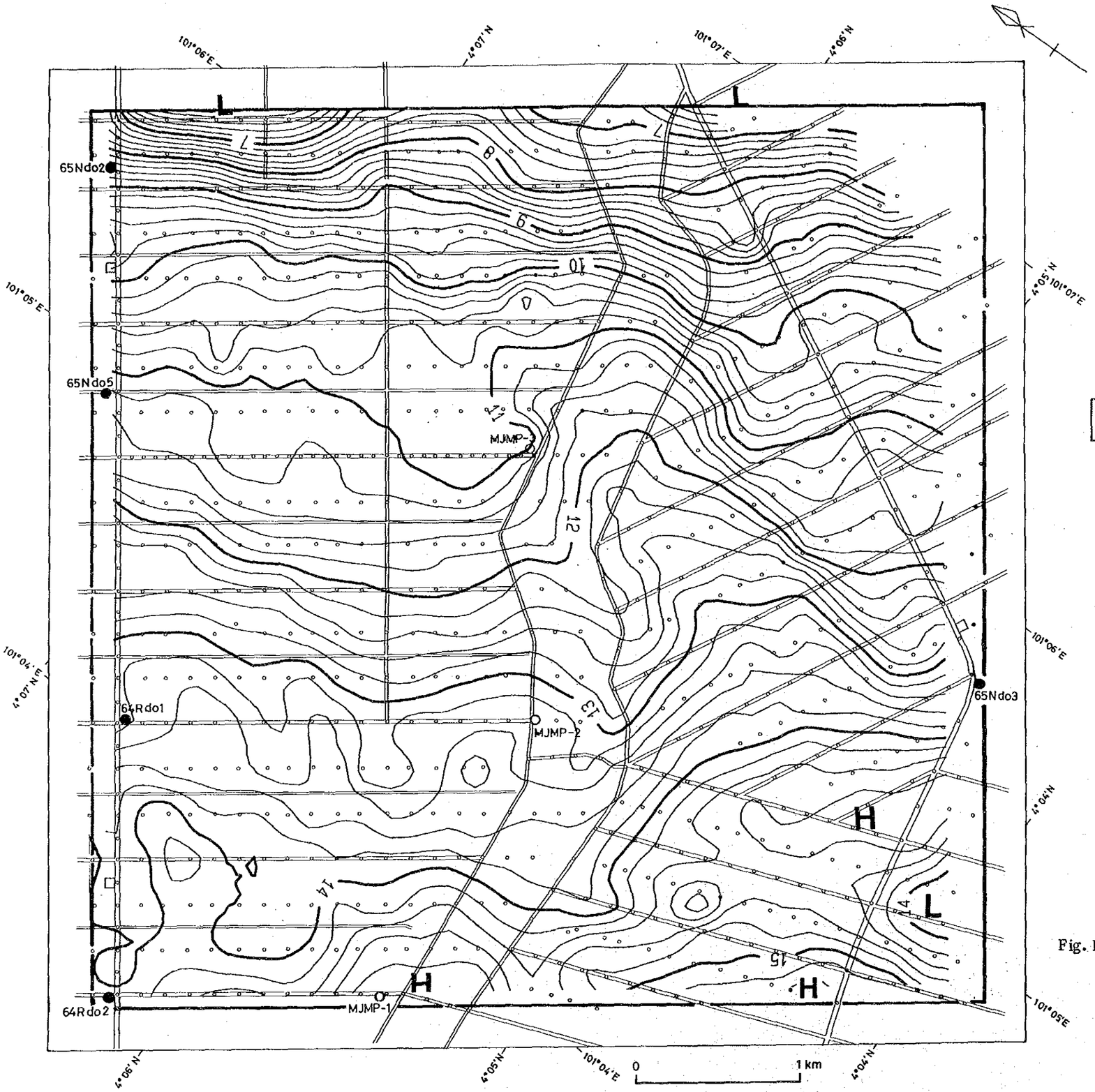

Fig. III - 2 - 10 Bouguer anomaly map (assumend density of 2.0 g/m^3)

Bouguer anomaly map (without topographical corrections) used for the regional gravity survey, now being conducted by Malaysia, clearly shows a regional gravity trend in which the gravity value decreases from the southwestern part of the area toward the northeastern part. This trend agrees with the results of this survey.

2-3-2 Power Spectral Analysis

A power spectral analysis was conducted for the Bouguer anomaly map by assuming the density as 1.8 g/cm^3. The results were as shown in Fig. III-2-11.

Separation into three bands: noise, residual and regional was effected from the distribution of power spectra. (1) Noise is represented by the frequency band with wavelengths of 0 to 520 m and reflects a noise structure in the shallow part of the ground surface. (2) The residual is represented by a frequency band with wavelengths of 520 to 2720 m and reflects the basement structure in this area. (3) The regional is represented by a frequency band of more than 2720 m and reflects the regional trend.

A gravity anomaly map (residual gravity anomaly map) for the band (2) believed to be most important in studying the basement structure in this area was prepared. It is shown in Fig. III-2-12. The gravity anomaly map for the band (3) is included in the Appendix.

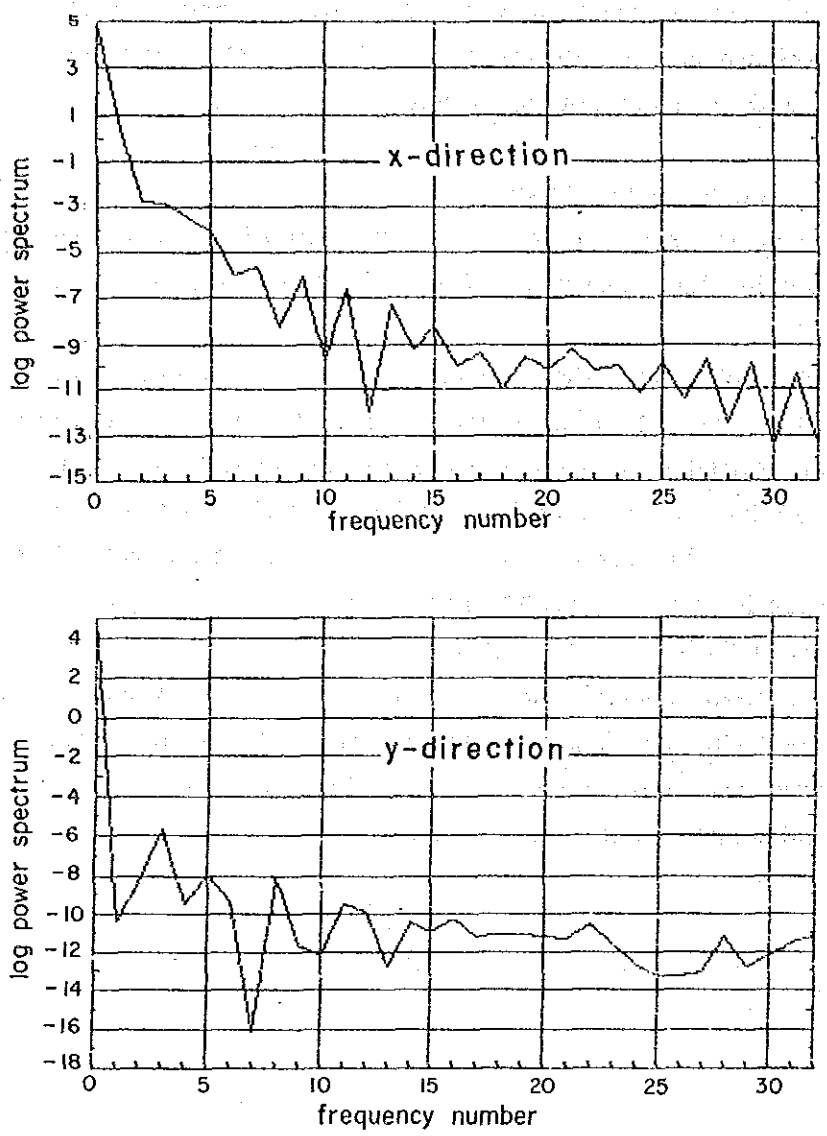

Fig. III - 2 - 11 Power spectral chart

2-3-3 Residual Gravity Anomaly Map

The residual gravity anomaly map is a Bouguer anomaly map minus the noise structure and the regional trend and is the gravity map that best reflects the basement structure in the survey area. It is shown in Fig. III-2-12.

In this map, the gravity value changes within the range of only about 3 mgal from -2 mgal to +0.9 mgal but high/low gravity anomalies indistinct in the Bouguer anomaly map are distinctly extracted in it. The NW-SE and N-S system ares prevalent along the directions of gravity contour lines. In this map, more than 0.2 mgal is termed as high gravity anomaly and less than -0.2 mgal is termed as low gravity anomaly.

It is presumed that the high gravity anomaly and the low gravity anomaly reflect, respectively, a crest and a hollow in the basement.

High gravity anomalies are distributed zonally from the northeastern half (H_1 and H_3) of the area and its central part (H_1) to the southern part (H_2) and the southwestern end (H_4 and H_5). Of these high gravity anomalies, the H_1 anomaly (about 1 km east of the MJMP-3 hole) shows the largest gravity value: +0.9 mgal.

Meanwhile, low gravity anomalies are distributed zonally in the northeastern end (L_1) of the area, its central part (L_2), the eastern part of the center (L_3) and the southern end (L_4) of the area. Of these low gravity anomalies, the anomaly at L_1 shows the smallest gravity value: -2 mgal. Particularly, the gravity value at L_1 tends to decrease furthermore toward northeast.

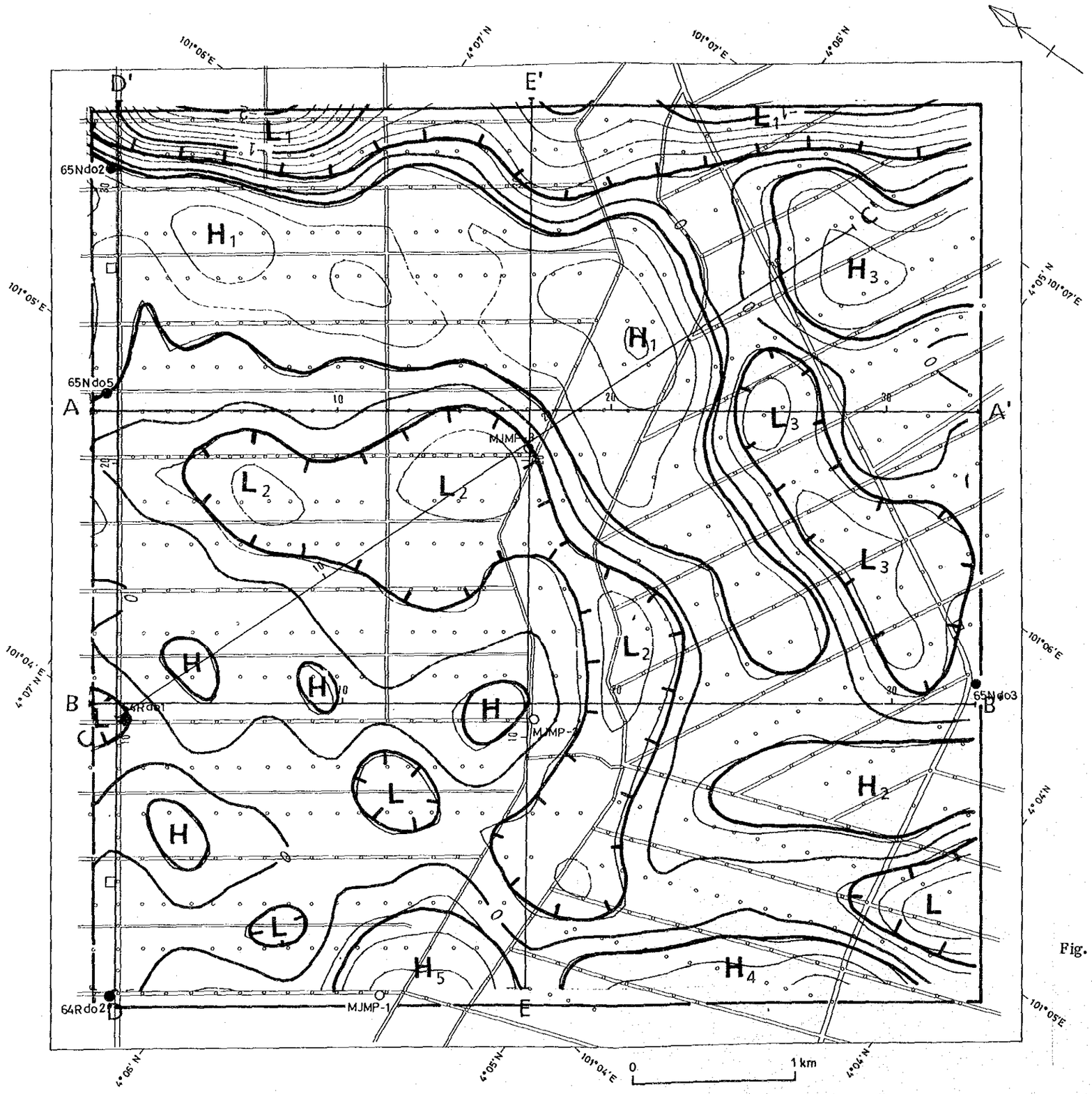

LEGEND

- Geophysical survey area (gravity method)
- Gravity point measured in this phase
- H — Gravity high
- L — Gravity low
- B—B' Section line
- Drilling site conducted by MMAJ in this phase
- Previous drilling site conducted by G.S. Malaysia
- Gravity anomalies in mgals

Fig. III - 2 - 12 Residual gravity anomaly map

2-3-4 3-Dimensional Structural Analysis Map

Three-dimensional structural analysis was conducted for the purpose of determining depth distribution in the basement structure from the residual gravity anomaly map. In the analysis, computation was made for four types of density differences and boundary surface mean depths. A most suitable map was decided from the comparison of the results of computation for each density and the previous drill data that in this survey area. This map is the three-dimensional structural analysis map by a density difference of 0.75 g/cm^3 and a mean depth of 75 m (Fig. III-2-13). In this report, computation results by a density difference of 0.70 g/cm^3 and a mean depth of 70 m and by a density difference of 0.80 g/cm^3 and a mean depth of 80 m are also shown (Fig. III-2-14 and Fig. III-2-15). Differences between computed basement depths from the ground surface and previous drill basement depths are shown in Table III-2-6.

The three-dimensional structural analysis map by a density difference of 0.75 g/cm^3 and a mean depth of 75 m is described below.

In this map, the irregularity in the gravity basement corresponds to the low/high gravity anomalies found from the residual gravity anomaly map (Fig. III-2-12). The gravity basement is shallowest: -40 m from the surface by high gravity anomaly H_1 and deepest at -160 m by low gravity anomaly L_1.

The gravity basement at high gravity anomalies (H_1-H_5) is shallow: -40 m -50 m at H_1 and H_3 but is deeper in the southern direction and, at H_2, it is distributed deeper than -60 m. But at the southwestern and (H_4, H_5), it becomes shallow again to the level of -40 m. Meanwhile, the gravity basement at low gravity anomalies (L_1-L_4) is deepest at level of -160 m at $L_1$and is relatively shallow at level of -90 m to level of -100 m at L_2-L_4. It is believed that in the vicinities of L_1 and H_1 as well as in L_1 and H_3, included in these high/low gravity anomalies, the gravity basement is sunken in the NE direction by 80-110 m. So, tectonic lines governing gravity basement structure are presumed to exist in these vicinities.

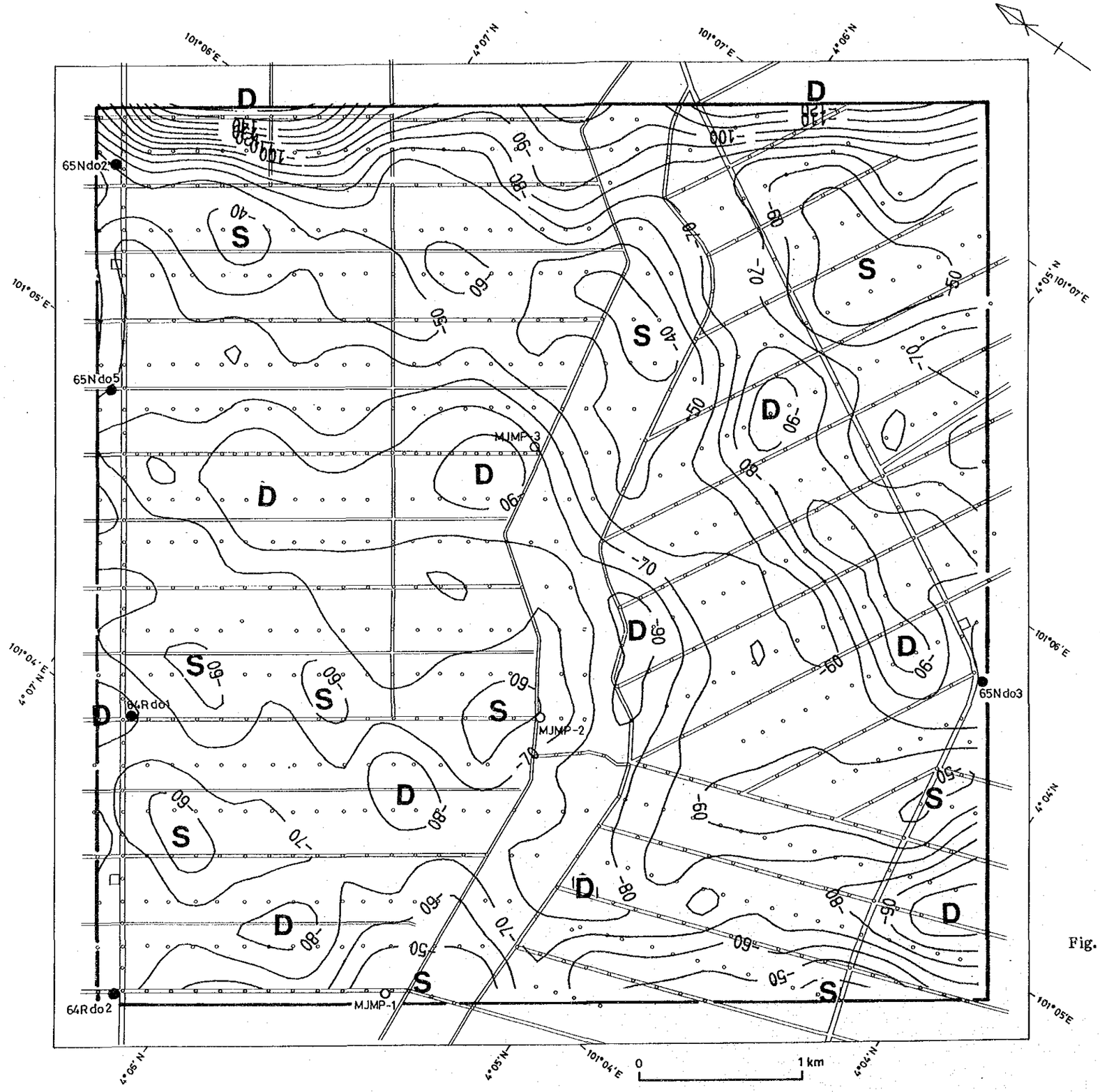

LEGEND

- Geophysical survey area (gravity method)
- o Gravity point measured in this phase
- S Peak of shallowest gravity basement
- D Bottom of deepest gravity basement
- o Drilling site conduted by MMAJ in this phase
- ● Previous drilling site conducted by G.S. Malaysia
- -60 -70 -80 Depth of gravity basement in m

Fig. III - 2 - 13 Structural map based on 3-d analysis (density difference 0.70 g/cm^3, mean depth 70m)

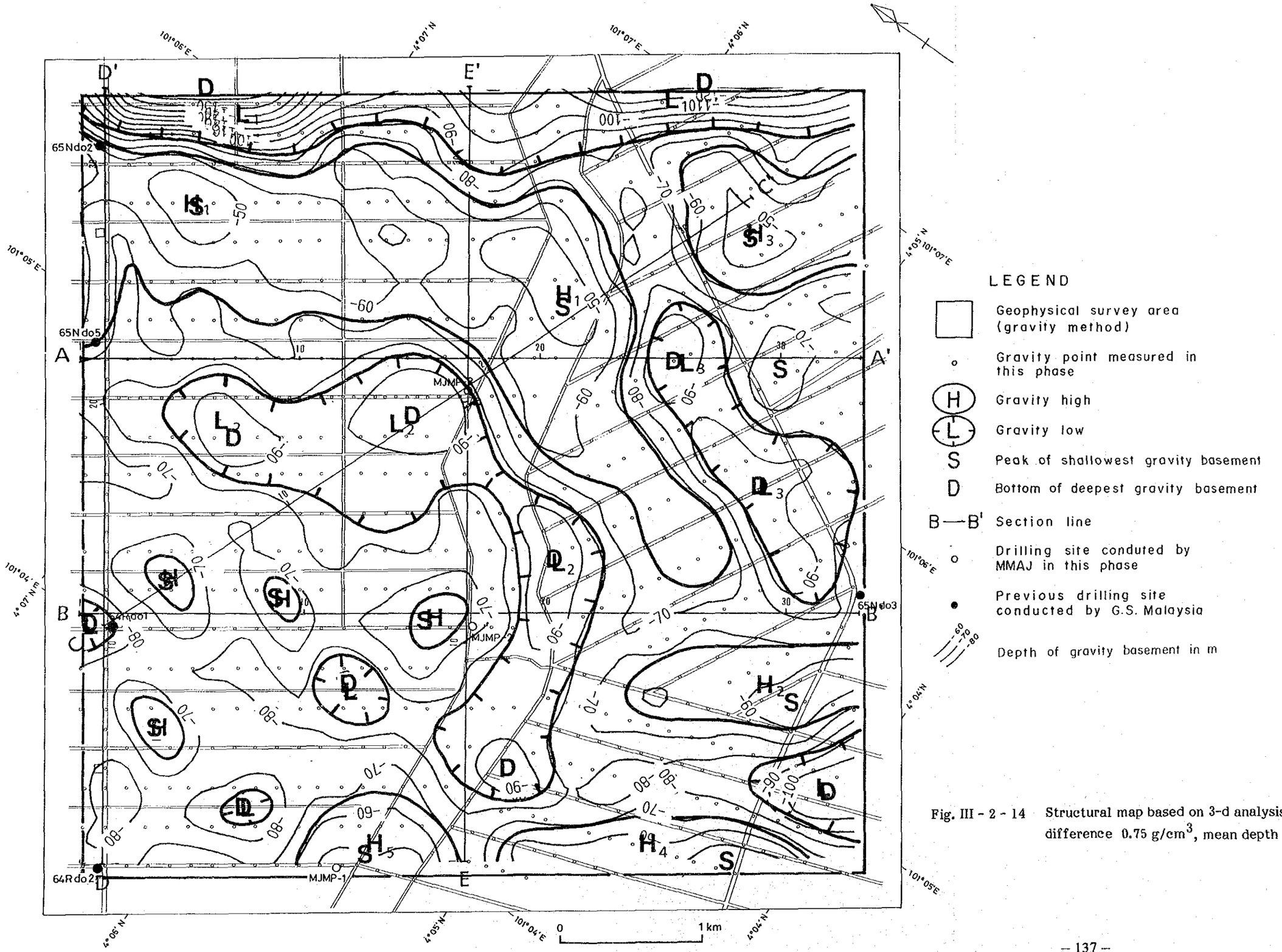

LEGEND

- Geophysical survey area (gravity method)
- Gravity point measured in this phase
- H — Gravity high
- L — Gravity low
- S — Peak of shallowest gravity basement
- D — Bottom of deepest gravity basement
- B—B' Section line
- Drilling site conduted by MMAJ in this phase
- Previous drilling site conducted by G.S. Malaysia
- Depth of gravity basement in m

Fig. III - 2 - 14 Structural map based on 3-d analysis (density difference 0.75 g/cm^3, mean depth 75m)

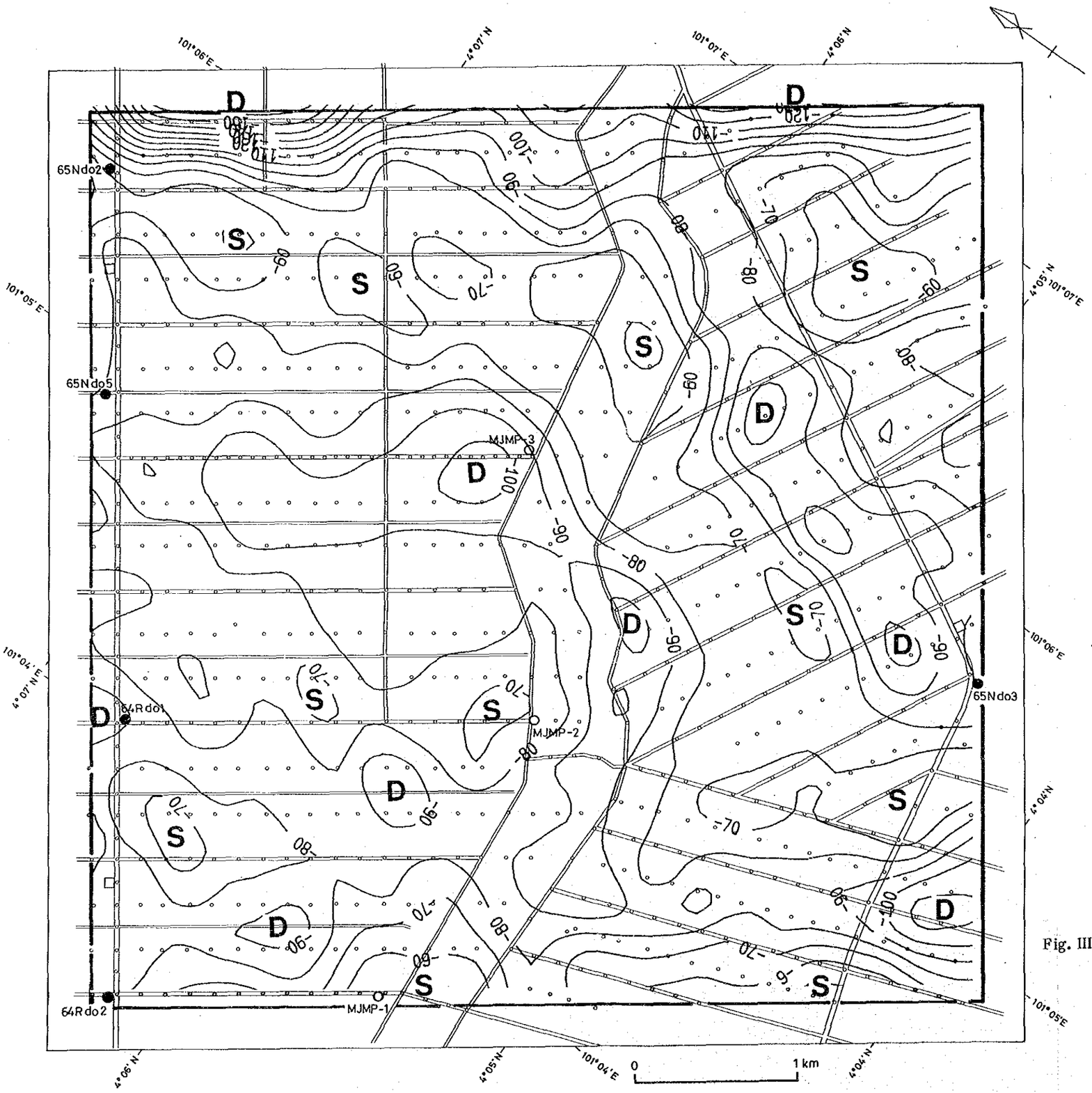

LEGEND

- Geophysical survey area (gravity method)
- ° Gravity point measured in this phase
- S Peak of shallowest gravity basement
- D Bottom of deepest gravity basement
- ° Drilling site conduted by MMAJ in this phase
- ● Previous drilling site conducted by G.S. Malaysia
- -60 -70 -80 Depth of gravity basement in m

Fig. III - 2 - 15 Structural map based on 3-d analysis (density difference 0.80 g/cm^3, mean depth 80m)

The table comparing gravity basement depths and drill data is shown in Table III-2-6.

In this survey, computation was made of four types of density differences (a, b, c and d) and mean depths.

a: density difference 0.60 g/cm^3, mean depth 50 m

b: density difference 0.70 g/cm^3, mean depth 70 m

c: density difference 0.75 g/cm^3, mean depth 75 m

d: density difference 0.80 g/cm^3, mean depth 80 m

Eight holes: 64Rd02, 64Rd01, 65Nd05, 65Nd02, MJMP-1, MJMP-2, MJMP-3 and 65Nd03 were drilled in the survey area. Of these eight, 64Rd02, 64Rd01, 65Nd05 are nearly approximate to the case of "c" with differences of less than 10 m. 65Nd02 and MJMP-2 are approximate to the case of "d" with differences of less than -10 m. MJMP-3 and 65Nd03 agree well with the case of "a" with differences of +4 m but their quaternary densities are somewhat larger. The increase of the quaternary densities if presumed to be due to coarse grained gravel. The MJMP-1 hole is not approximate in any case. This hole is located in a high gravity anomaly (H_5). So, it presumably was drilled in a depression of a local gravity basement.

2-3-5 2-Dimensional Analysis Map

This map was prepared to assess the distribution of bedrock depths in the survey area. Five cross-section lines were set up passing through each drilled hole, as indicated in Fig. III-2-12. Filtering results and results of three-dimensional structural analysis (density difference 0.75 g/cm^3, mean depth 75 m) are illustrated for each section.

1) Section A-A' (Fig. III-2-16)

This is a NW-SE section crossing the low gravity anomalies of L_2 and L_3 and the high gravity anomaly of H_1 and passing through 65Nd05 and MJMP-3.

The gravity basement is relatively deep: -60 m to - 80 m in elevation but basement projections are found near No. 19 to No. 22 and the top-surface depth is shallow: -30m -50 m in elevation. Meanwhile, gravity basement depressions are found near No. 15 and No. 25. Gravity basement depth in this vicinity is -80 m.

Table. Ⅲ-2-6 Comparison of depth of basement between the geological and gravity results

S No.	Hole		Depth of gravity basement							
			a		b		c		d	
	Name	Depth(m)	Depth(m)	ΔD(m)	Depth(m)	ΔD(m)	Depth(m)	ΔD(m)	Depth(m)	ΔD(m)
1	64RdO2	-67	-51	-16	-72	5*	-76	9	-83	16
2	64RdO1	-84	-64	-20	-82	-2*	-86	2*	-92	8
3	65NdO5	-63	-43	-20	-61	-2*	-66	3	-73	10
4	65NdO2	-63	-14	-49	-45	-18	-50	-13	-55	-8*
5	MJMP-1	-98	-20	-78	-46	-52	-49	-49	-58	-40
6	MJMP-2	-76	-40	-36	-60	-16	-68	-8	-71	-5*
7	MJMP-3	-62	-64	2*	-84	22	-90	28	-93	31
8	65NdO3	-57	-53	-4*	-72	15	-75	18	-81	24

a : Density difference 0.60g/cm³, mean depth 50m
b : Density difference 0.70g/cm³, mean depth 70m
c : Density difference 0.75g/cm³, mean depth 75m
d : Density difference 0.80g/cm³, mean depth 80m

Depth of gravity basement is the depth of basement determined by gravity survey. Minus (-) sign mean downward from the surface. ΔD means the difference in depth of basement between the geological and gravity results. Sign * shows the miniumum difference of basement depth between the geological and geophysical results.

2) Section B-B' (Fig. III-2-17)

This is a NW-SE section crossing the low gravity anomaly of L_2 and passing through the drilled holes of 64Rd01, MJMP-2 and 65Nd03.

The gravity basement is somewhat shallow: -50 m to -60 m in elevation and, at No. 20 to No. 21, greatly sinks to -80m in elevation, presenting depressions in the gravity basement.

3) Section C-C' (Fig. III-2-18)

This is an E-W section crossing the low gravity anomaly of L_2 and the high gravity anomalies of H_1 and H_3 and passing through 64Rd01 and MJMP-3.

The gravity basement gradually increases in depth from -60 m to -80 m in elevation from the western part of the section to its central part but becomes gradually shallower toward the eastern part of the section. In the vicinities of No. 24 to No. 25 and No. 32 from the western part of the section to its central part, it is shallower (-30 m in elevation) than it is anywhere else in the survey area. Hollows in the gravity basement are found in the vicinities of No. 16 to No. 18 and No. 27.

4) Section D-D' (Fig. III-2-19)

This is the NE-SW section crossing the high/low gravity anomalies of H_1 and L_1 in the northeastern part of the section and passing through 64Rd02, 64Rd01, 65Nd05 and 65Nd02.

The gravity basement is somewhat deep: -60 m to -70 m in elevation from the southwestern part of the section to its central part but, in the northeastern part of the section, it is shallow: -30 m in elevation in the vicinities of No. 29 to No. 30. At the northeastern end of the section, it suddenly sinks to -100 m in elevation. From these facts, fault tectonic lines presumably exist at the northeastern end of the section. Meanwhile, hollows in the gravity basement are found in the vicinity of No. 11 and the vicinities of No. 20 to No. 21 but they are believed to be small because of the small height difference in the basement.

5) Section E-E' (Fig. III-2-20)

This is an NE-SW section crossing the low gravity anomaly of L_2 and the high gravity anomaly of H_1 and passing though MJMP-2 and MJMP-3.

As a whole, the gravity basement is relatively deep: -60 m to -80 m in elevation but in the vicinities of No. 24 to No. 27, it is shallow: -40 m in elevation. In the northeastern part of the section, the gravity basement suddenly sinks from -40 m in elevation to - 90 m. So, it can be presumed that tectonic lines reflecting faults exist there. Hollows in the gravity basement are found at No. 4 to No. 6 and No. 17 to No. 20.

2-4 Discussion

The purpose of the geophysical exploration (gravity method) in this area was to assess the extent and continuity of hollows in a basement with high prospects as a favorable basin for tin deposition by assessing the basement structure from gravity distribution in the survey area.

The followings are the discussions of consolidated results of the survey (Fig. III-2-21).

1) NW-SE tectonic lines presumed to represent faults were detected in the northeastern part of this area. These tectonis lines govern the basement structure and the throw is presumed to exceed 100 m.

2) The Bouguer anomaly map for this area shows the regional trend the gravity value decreases from the southwestern part of the area toward its northeastern part. Clear high/low gravity anomalies were extracted by eliminating the regional trend and the noise structure from Bouguer anomaly map by power spectral analysis and frequency band separation.

3) In this area, high gravity anomalies were found from the five places of H_1 through H_5. In these high gravity anomalous zones, the basement is presumed to be distributed shallowly from the ground surface. The results of a three-dimensional structural analysis show that the gravity basement at H_1 through H_5 is distributed at depths from -40 m to more than -60 m.

4) Low gravity anomalies in this area were detected at four places: L_1 through L_4. In these low gravity anomalous zones, reversely to high gravity anomalies, the basement is believed to be depressed and deep. From three-dimentional structural analysis, low gravity anomalies are at great depths: more than -160 m at L_1 and -90 m to -100 m at L_2 to L_4.

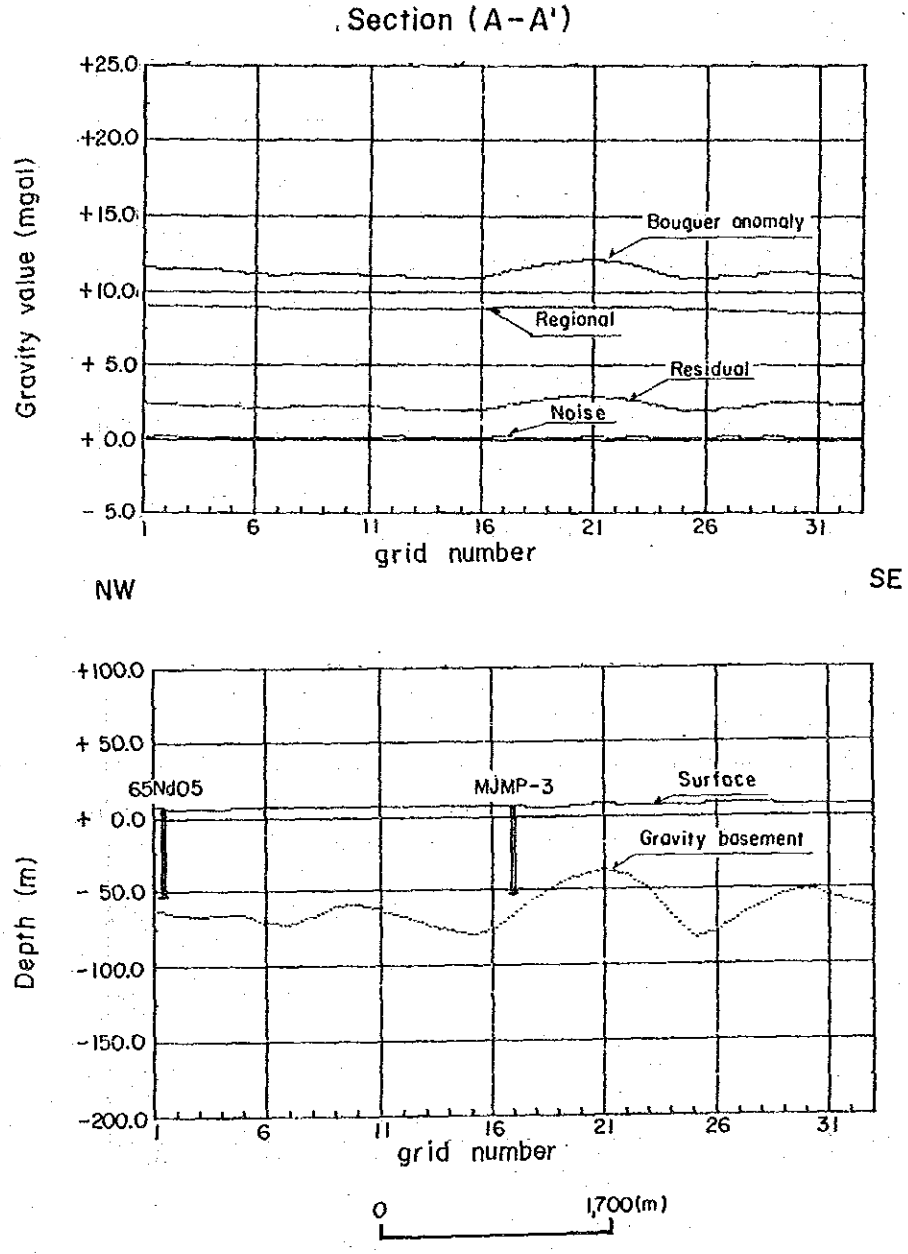

Fig. III - 2 - 16 Section analysis of 2-layered density structure (A-A')

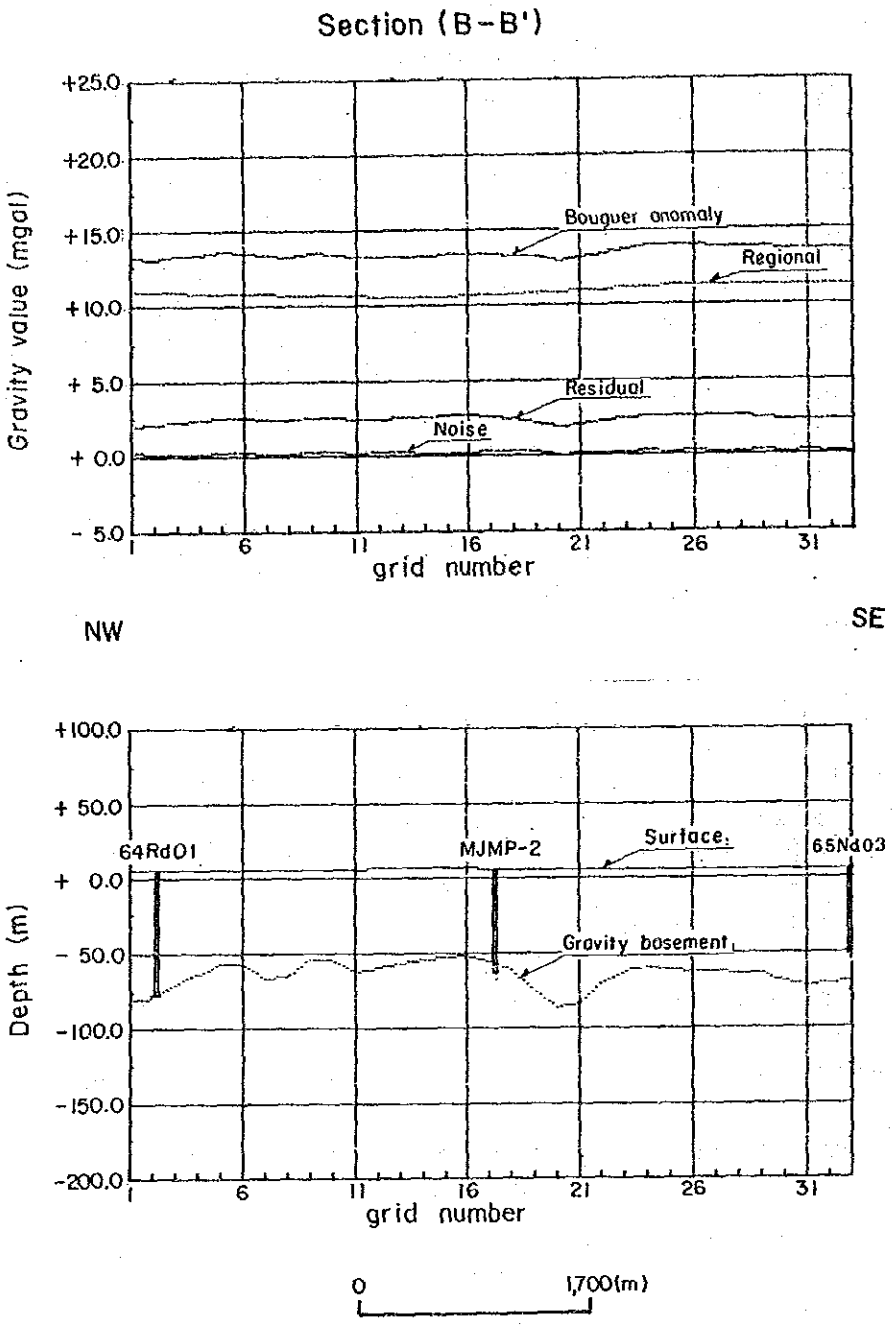

Fig. III - 2 - 17 Section analysis of 2-layered density structure (B-B')

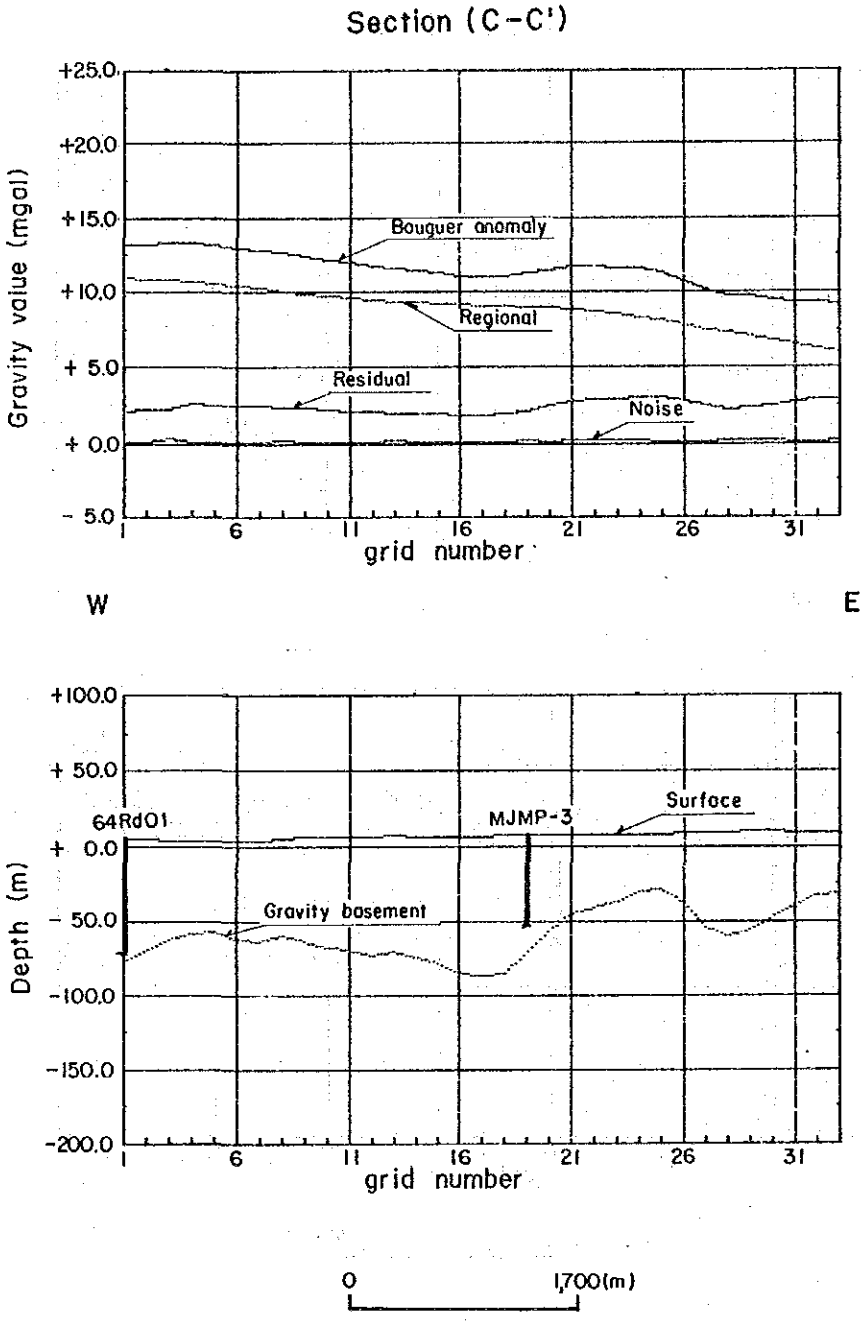

Fig. III - 2 - 18 Section analysis of 2-layered density structure (C-C')

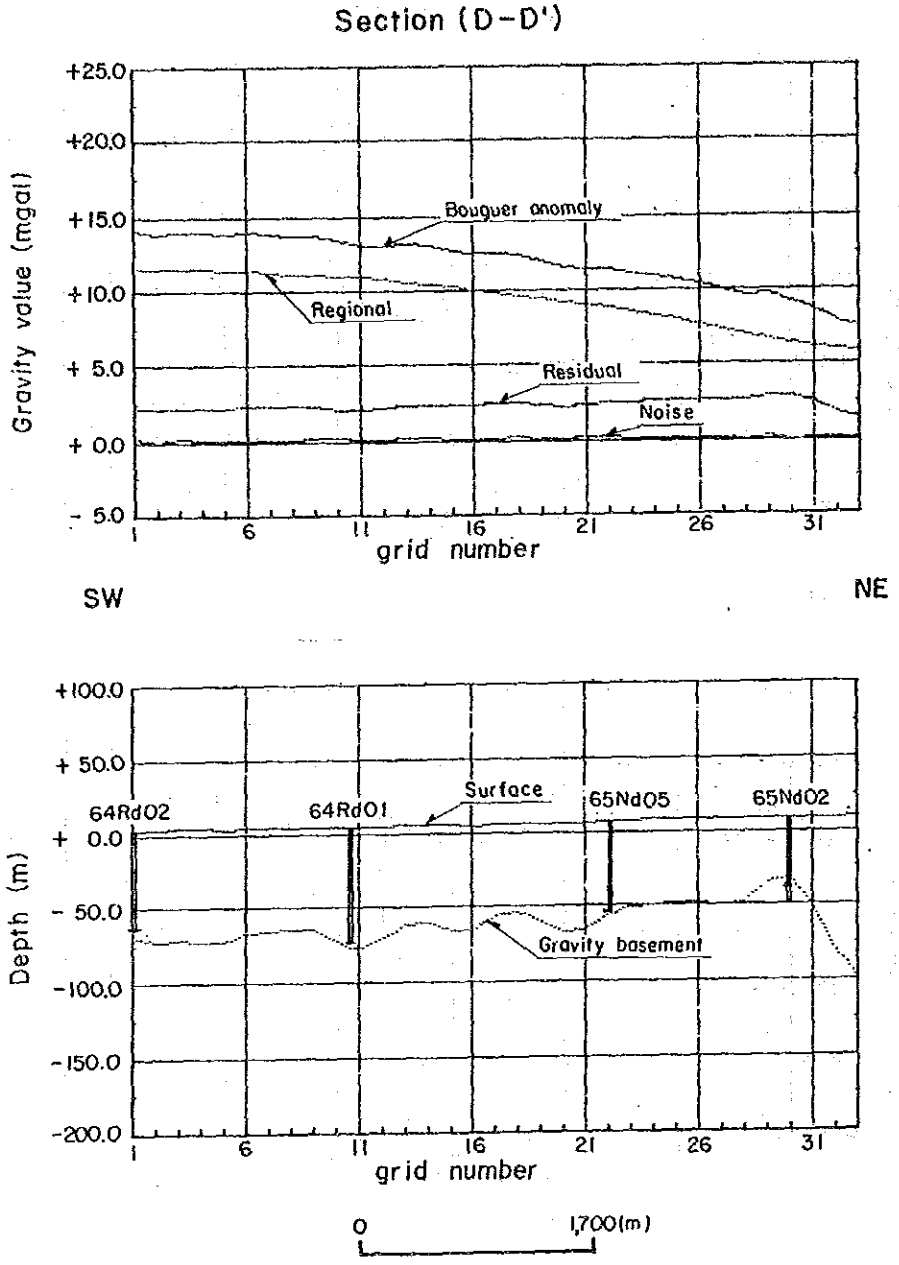

Fig. III - 2 - 19 Section analysis of 2-layered density structure (D-D')

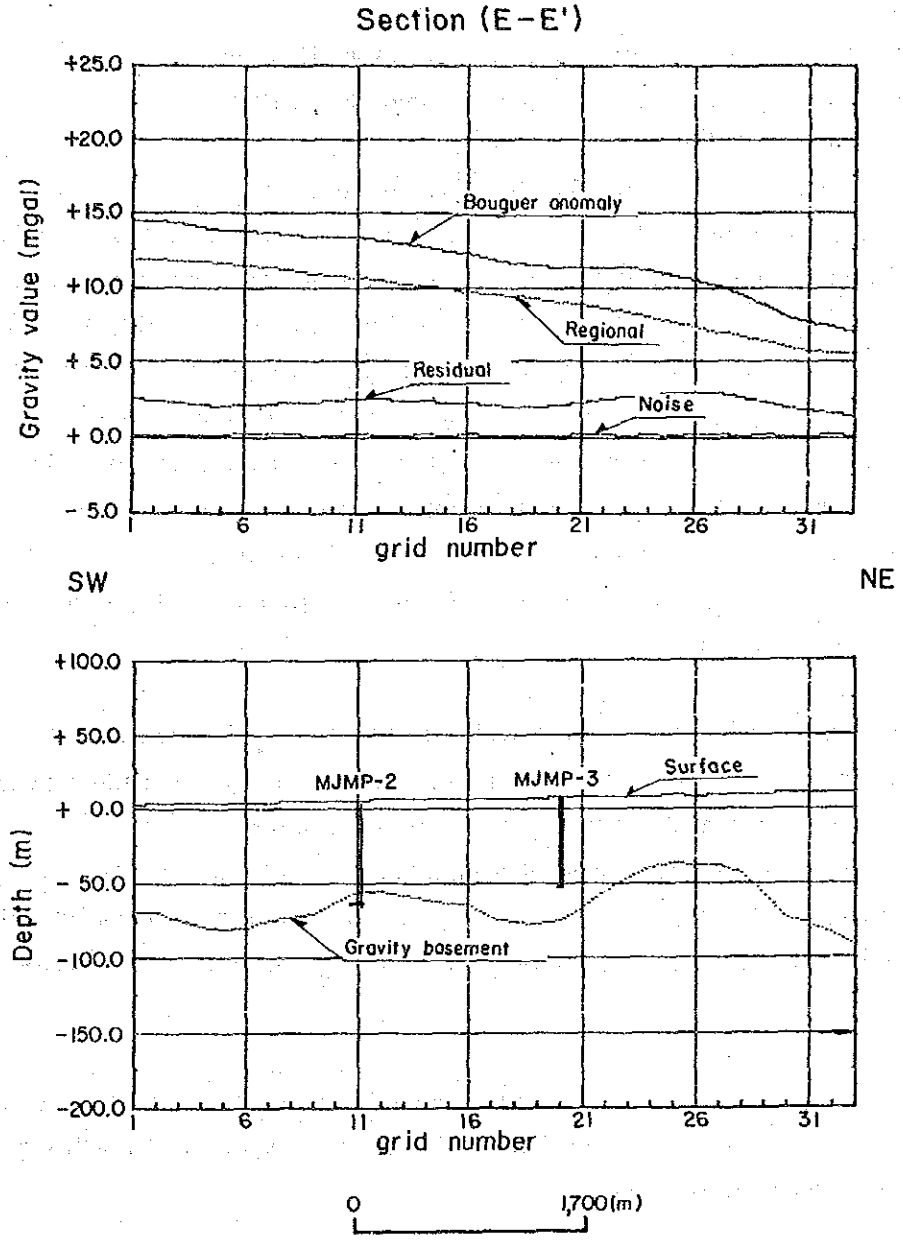

Fig. III - 2 - 20 Section analysis of 2-layered density structure (E-E')

5) In this survey, comparison was made between gravity basement depths by four types of density differences and mean depths (a, b, c and d) and each drill data.

a: density difference 0.60 g/cm^3, mean depth 50 m

b: density difference 0.70 g/cm^3, mean depth 70 m

c: density difference 0.75 g/cm^3, mean depth 75 m

d: density difference 0.80 g/cm^3, mean depth 80 m

Eight holes: 64Rd02, 64Rd01, 65Nd05, 65Nd02, MJMP-1, MJMP-2, MJMP-3 and 65Nd03 were drilled in the survey area. Of these eight, 64Rd02, 64Rd01, 65Nd05 are nearly approximate to the case of "c" with differences of less than 10 m. 65Nd02 and MJMP-2 are approximate to the case of "d" with differences of less than -10 m. MJMP-3 and 65Nd03 agree well with the case of "a" with differences of +4 m but their quaternary densities are somewhat larger. This is presumed to be due to coarse grained gravel. The MJMP-1 hole is not approximate in any case. The hole is located in a high gravity anomaly (H_5). So, it presumably was drilled in a depression of a local gravity basement.

6) The drilled holes were compared with respect to tin ore width percent (thickness x assay, unit m kg/m^3) and gravity distribution (residual gravity anomaly map). The results were as shown in Table III-2-7.

In this table, the existence of a high tin ore width percent (1.5 or over) in the center of the high gravity anomaly and it periphery was confirmed by drilling conducted in the area surrounded by high gravity anomaly distribution zones.

7) The depression in the basement is considered to be basically important as a favorable basin of tin deposition. However, prospecting by drilling has not yet been conducted there.

8) It is, therefore, likely that the relationship between the gravity distribution and the favorable basin of tin deposition in the depression of the basement will be clarified by conducting prospecting by drilling there.

Table. Ⅲ-2-7 Comparative results from drill holes, Width percent (SnO_2) and gravity anomalies

SNo.	Hole		Width percent (SnO_2) (m・kg/ m^3)	Hole location in relation to gravity anomalies
	Name	Depth(m)		
1	64Rd02	67	0.72 (59.4～60.9m) (64.0～65.5m)	Boundary between an anomaly high and low
2	64Rd01	84	2.30 (70.1～76.1m)	Boundary between an anomaly high and low
3	65Nd05	63	1.94 (54.9～56.4m)	Boundary between an anomaly high and low
4	65Nd02	63	4.15 (57.9～62.4m)	Middle of an anomaly high
5	MJMP-1	98	3.67 (83.8～88.3m)	Middle of an anomaly high
6	MJMP-2	76	3.01 (64.0～65.5m) (68.6～73.1m)	Middle of an anomaly high
7	MJMP-3	62	2.42 (57.9～60.9m)	Boundary between an anomaly high and low
8	65Nd03	57	0.17 (53.3～56.3m)	Boundary between an anomaly high and low

The value in parenthesis shows the depth in meter from the surface.

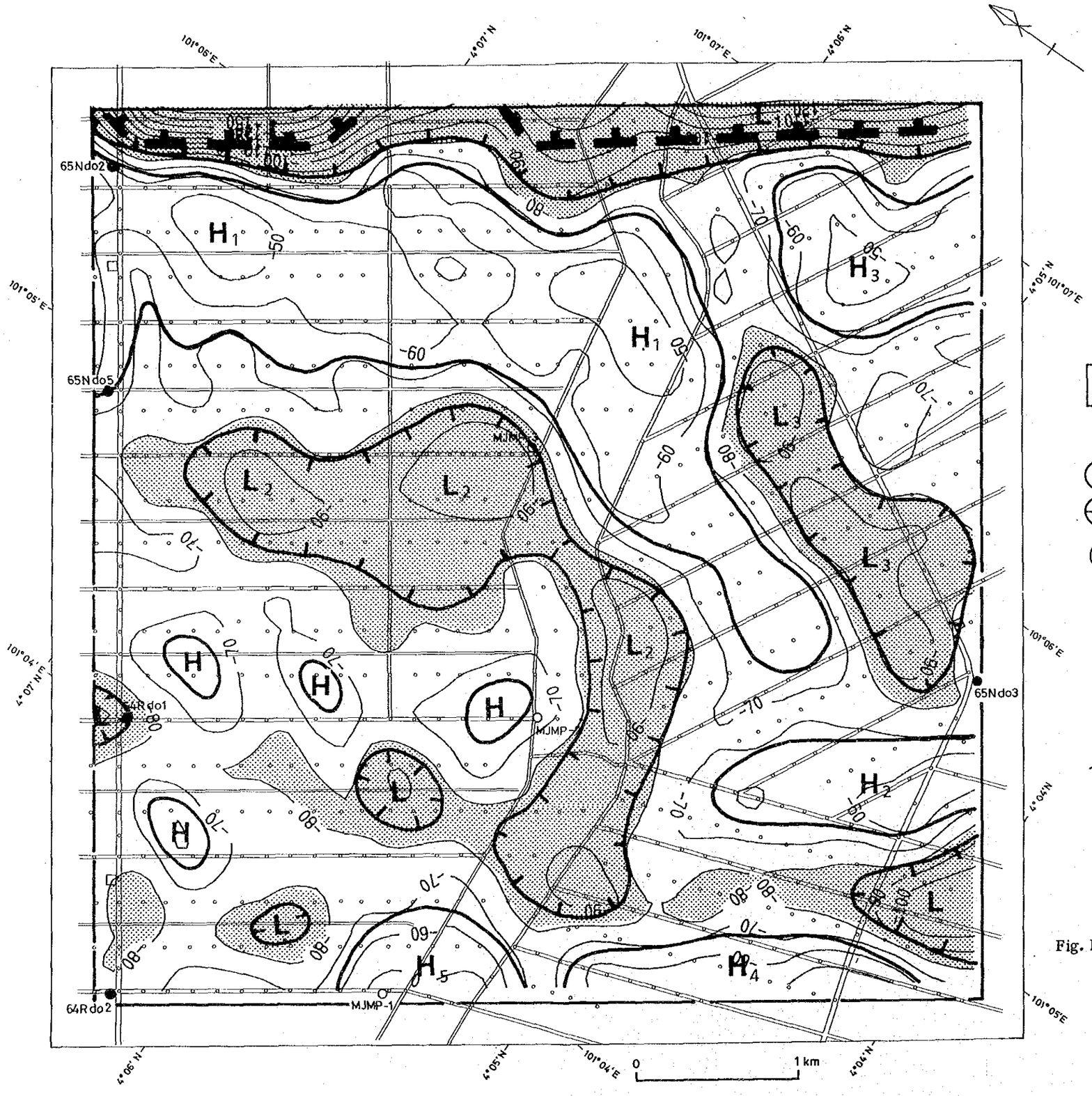

LEGEND

- Geophysical survey area (gravity method)
- Gravity point measured in this phase
- H — Gravity high
- L — Gravity low
- Deepest area of gravity basement (less than -80m from the surface)
- Drilling site conducted by MMAJ in this phase
- Previous drilling site conducted by G.S. Malaysia
- Fault estimated by gravity survey results
- -60 -70 -80 — Depth of gravity basement in m

Fig. III - 2 - 21 Gravity interpretation map